8-2013

A GIS-based Multi-objective Optimization of a Lignocellulosic Biomass Supply Chain: A Case Study in Tennessee

Zidong Wang
zwang36@utk.edu

To the Graduate Council:

I am submitting herewith a thesis written by Zidong Wang entitled "A GIS-based Multi-objective Optimization of a Lignocellulosic Biomass Supply Chain: A Case Study in Tennessee." I have examined the final electronic copy of this thesis for form and content and recommend that it be accepted in partial fulfillment of the requirements for the degree of Master of Science, with a major in Agricultural Economics.

Tun-Hsiang E. Yu, Major Professor

We have read this thesis and recommend its acceptance:

Burton C. English, James A. Larson

Accepted for the Council:
Dixie L. Thompson

Vice Provost and Dean of the Graduate School

(Original signatures are on file with official student records.)

A GIS-based Multi-objective Optimization of a Lignocellulosic Biomass Supply Chain: A Case Study in Tennessee

A Thesis Presented for the
Master of Science
Degree
The University of Tennessee, Knoxville

Zidong Wang
August 2013

Acknowledgements

First of all I would like to thank my major advisor, Dr. Edward Yu for the continual instruction and support during my master study. I would like to thank Dr. Burton English for his priceless encouragement and suggestions. Also I want to thanks Dr. James Larson, whose constructive guidance enabled me to have a deep understanding in this area. This thesis is a much better work thanks to their supervision.

I would like to extend my gratitude to Yuan Gao from IMF, Dr. Bruce McCarl from Texas A&M University, Dr. George Mavrotas from The National Technical University of Athens, Greece, Dr. Michael Bussieck, Dr. Toni Lastusilta from GAMS Development Corporation and Dr. Cindy Keough from Colorado State University for their patiently help and useful suggestions in my study.

I have a great time during my master study here thanks to all my classmates in the Department. They are Tingting Tong, Haijing Zhuang, Yanghao Wang, Tianpeng Zhou, Shikha Chugh, Carey Wolanin, Tan Watcharaanantapong, Olga Khaliukova and Eric Bisangwa. Special thanks are given to Stacy Williams who always give me a hand whenever I need help.

I also want to thank all my friends, especially my girlfriend Qiumin Ma, for being always supportive and understanding. At last, I would like to thank my family, especially my parents and grandparents. I am the luckiest to have you being around me, supporting me and guiding me unconditionally.

Abstract

To achieve an economically and environmentally sustainable lignocellulosic biomass (LCB)-based biofuel industry sector, the design and location of a sustainable LCB supply chain is important. In this study, a multi-objective optimization model integrated with high-resolution geographical data was developed to examine the optimal switchgrass supply chain for a potential biorefinery in Tennessee, specifically evaluating the potential tradeoffs between the objectives of minimizing plant-gate cost and GHG emissions from the switchgrass supply chain. The key findings of this study are as follows: both plant-gate feedstock cost and GHG emissions were sensitive to the type of land converted into switchgrass production, the type of land use change also affected the density of the feedstock supply region due to the spatial heterogeneity in the availability of different types of land, hence affecting transportation-related cost and GHG emissions, and a tradeoff relationship was discovered between cost and GHG emissions for the switchgrass supply chain, primarily driven by the type of land converted.

As a result of land use changes and transportation distances, the imputed cost to reduce one unit of GHG emissions was initially modest; however, the imputed cost increased considerably when the supply chain GHG emissions were further mitigated. This implied that the location of switchgrass production and the resulting changes in crop production should be considered in targeting government incentives to encourage switchgrass-based biofuel production in the state and the southeastern region. Sensitivity analyses indicated that the dry matter loss (DML) decomposition, if considered as a source of GHG emissions, would considerably increase the supply chain GHG emissions. Different harvest and storage technology used in the feedstock supply chain altered the DML rate and corresponding GHG emissions however did not change the tradeoffs between the two objectives significantly. The consideration

of GHG emissions from cattle relocation, on the other hand, appears to reduce the GHG emission level of the supply chain to a great extent and change the tradeoff relation between the two objectives.

Table of Contents

List of Tables

List of Figures

Chapter 1 Introduction

Concerns about rising fuel prices and climate change have stimulated public and government interest in finding more sustainable energy sources such as solar, wind, and biofuel. Specifically, the development of a biofuel industrial sector has been widely recognized as one potential alternative to reduce fossil fuel usage and vehicle emissions (Demirbas, 2007). Biofuel production is primarily generated from conventional feedstocks, e.g. corn grain in the U.S., given their rich sugar or starch content (Crago et al., 2010). With the increasing concern about the linkage between biofuel production and food prices, more attention has been directed to non-food biofuel feedstocks.

Lignocellulosic biomass (LCB) has been regarded as a promising non-food feedstock for biofuel production in the United States (Chum and Overend, 2001). Compared with conventional feedstocks such as corn grain, LCB feedstocks are potentially abundant and less linked to food market. LCB feedstocks offer additional benefits in terms of soil erosion reduction and increased biodiversity (Smeets et al., 2009). Thus, the Renewable Fuel Standard (RFS), an important part of the Energy Independence and Security Act (EISA) of 2007, mandated the production of 500 million gallons of LCB-based biofuel in 2012, 1 billion gallons in 2013, and at least 16 billion in 2022 to be used by the transportation sector (U.S. Congress, 2007).

Notwithstanding the national mandate, the expected biofuel production from LCB feedstock is only 5 million gallons in 2013. Production is expected to increase to 250 million gallons by 2015 with the establishment of more biorefinery plants, according to a recent U.S. Energy Information Administration report (EIA, 2013). One cause of the substantial gap between the actual volumes of LCB-based biofuel production and the mandate is the delivery cost of LCB feedstocks (Bansal et al., 2013). The LCB supply chain encompasses the flow of feedstock from field to the biorefinery gate, including production, harvest/collection, storage, and transportation (Sokhansanj et al., 2006). The design of LCB supply chain has great implications to the economic and environmental sustainability of biofuel industry (Hess et al., 2003). Specifically, the LCB supply chain can constitute 20-50% of the total biofuel production cost (Hess et al., 2007; Eksioglu et al., 2009). Also, activities in an LCB supply chain e.g. change in land use, fertilizer application, and feedstock transportation, produce GHG emissions (Qin et al., 2011; Adler et al., 2007; Yu et al., 2013). Therefore, the economic and environmental performance of feedstock supply chain needs to be carefully studied when considering the development of a commercialized biofuel industrial sector.

When assessing the economic and/or environmental performance of the LCB supply chain, it is common to incorporate spatial information by using a geographical information system (GIS) (e.g. Graham et al. 1996a; Zhang et al., 2011), especially for the site-specific studies (e.g. Jappinen et al., 2011; Archer and Johnson, 2012). These studies analyzed the sustainability of single or multiple biofuel plants and the associated feedstock supply chains (e.g. Petrolia, 2008; Jappinen et al., 2013; Archer and Johnson, 2012) and their local influences, e.g. traffic and air quality (Yu et al. 2013). Those studies suggested that local geographical properties should be considered when evaluating the economic and environmental sustainability of an LCB supply chain. More precisely, the spatial variation in the availability of feedstock and production cost led to considerable differences in the supply chain costs between candidate locations (Noon et al., 2002). In addition, the quantity and quality of available feedstock could contribute to variations in GHG emissions produced from feedstock supply chains (Jappinen et al., 2011). Besides the local feedstock availability, the type of land use change also influenced the economic and environmental performance of an LCB supply chain as the conversion of different types of land to switchgrass leading to different opportunity costs and soil CO_2 emissions/sequestration (Qin et al., 2011; Kwon et al. 2013). In addition, the quality of local transportation network affected the average speed and hence the transportation cost and GHG emissions of a feedstock supply system.

Mathematical programming is a commonly adopted approach in site-specific studies to determine the location of the biorefinery and the optimal design of an LCB supply chain. The objectives of the mathematical models in many studies were optimizing economic factors such as cost minimization, net present value maximization, or profit maximization (Dunnett, et al. 2007; Kondili et al., 1993; Mas et al., 2010), whereas a few studies also considered both economic and environmental optimization in the decision criteria (Bernardi et al., 2012; Elia et al., 2011; Zhang et al., 2012). Local geographical information such as the spatial variation of feedstock yield and fuel demand was incorporated in the mathematical programming model to determine the optimal biorefinery site and feedstock supply chain (You et al. 2012). However, the type of land use change and local road network were usually neglected in multi-objective optimization studies of the LCB supply chain, despite the potential impact of land use change by crop type on GHG emissions (Kwon et al., 2013).

In this thesis, a case study was conducted to examine the sustainability of using switchgrass as a feedstock for biofuel production in Tennessee by considering both economic and environmental performance of the feedstock supply chain. Local land use change and road network data was incorporated. Switchgrass, a native perennial grass in North America, has long been regarded as a promising LCB feedstock for biofuel production. Studies have shown a higher yield of switchgrass in the humid subtropical climate of the Southeastern U.S. such as Tennessee than in other regions of U.S. (Gunderson et al., 2008). In Tennessee, a total of $70 million was allocated to the Tennessee Biofuel Initiative, a state-supported program to help the development of switchgrass-based biofuel industry. Consequently, a total of 5,100 acres of switchgrass land and a pilot cellulosic biorefinery were established (Jackson, 2012). Based on the progress of the biofuel program in Tennessee and the potential for commercial biofuel production in the future, this study aimed to provide valuable information about the key factors in the design of a sustainable switchgrass supply chain. The specific objectives of this study were twofold:

(1) Evaluate the key factors that influence the cost and GHG emissions of a switchgrass supply chain in Tennessee and evaluate the potential tradeoffs between economic and environmental performance in the switchgrass supply chain, and

(2) Determine the location of potential biorefinery and the associated switchgrass supply region and examine the relationship between the types of land used for conversion and the density of the switchgrass supply chain.

This study hypothesized that: (1) a tradeoff might exist between these two evaluated criterions and (2) the land conversion type influenced the biorefinery location and the density of the feedstock supply region.

Chapter 2 Literature Review

2.1 The LCB Supply Chain Design

The design of a sustainable LCB supply chain and efficient conversion technology has become the main focus of most current research efforts in biomass and bioenergy studies (Sharma et al., 2013). Studies indicated that the development of an LCB supply chain faced several challenges ranging from cultivation of biomass to feedstock collection and transportation (Rentizelas et al., 2009). For example, the scattered geographical distribution of biomass availability added considerably to cost during feedstock harvest, collection, and handling (Gold and Seuring, 2011); the limited harvest time for most LCB feedstocks led to off-season under-utilization of machinery and equipment (Dunnett et al., 2007); the low energy density of LCB feedstock and the limited capacity of carriers added considerable cost of feedstock transportation as well as potential social and environmental impacts (Gold and Seuring, 2011; Kumar et al., 2007). As the RFS is mandating 16 billion gallons of LCB biofuel for the transportation sector by 2022, the development of more sustainable LCB supply chains is a necessary prerequisite to the effort to fulfill the national target.

Recently, advanced tools and mathematical modeling have been used in the design of the LCB supply chain (Sharma et al., 2013). Mathematical modeling has been adopted to analyze the optimal supply chain design for product manufacturing, inventory management, and distribution (e.g. Cohen and Lee, 1998; Newhart et al. 1993; Voudouris and Consulting, 1996). Among the studies applying mathematical modeling in the LCB feedstock supply chain, many have focused on economic factors such as cost, net present value (NPV) or profit. For instance, Cundiff et al. (1997) conducted a case study in Piedmont County, South Carolina to examine the economic performance of a hypothetical bioethanol plant. Several switchgrass producers were considered, each with its own storage location. Cost estimates were provided for switchgrass loading, storage, transportation. Comparison of different storage methods was conducted. Dunnett et al. (2007) analyzed the economic sustainability of the LCB feedstock stock supply chain for a heat plant with a 20 MWth peak output. Agricultural land within 1,225 square km area was considered as a supply region, and the study indicated that land, cultivation and harvesting from the feedstock supply chain accounted for the major portion of the total cost.

Zhang et al. (2012) proposed a mixed integer linear programming (MILP) model to examine the potential development of a switchgrass-based bioethanol supply chain with supply chain cost minimization as its objective, suggesting that the demand for gasoline in North Dakota could be met if 61% of the marginal agricultural land was converted into switchgrass for biofuel production. Mas et al. (2010) added the uncertainties in market conditions when optimizing profit in the design and planning of biomass-based fuel supply networks for ethanol production. Two optimization criteria, i.e., profit maximization and risk minimization, were tested in their case study in northern Italy. Results from profit maximization indicated that biorefinery profitability was sensitive to the market price of Dried Distillers Grains with Solubles (DDGS). Results from risk minimization indicated that the investment of ethanol production would not be sustainable with a low DDGS selling price.

Previous studies have also indicated the potential influence of the LCB supply chain on the environment (Gold and Seuring, 2011; Bojarski et al., 2009) and social welfare (You et al., 2012). Additionally, a few exceptional cases have used a multi-objective approach to include other criteria, such as environmental quality or employment, which might influence the sustainability of a biorefinery in objective functions as well as on the basis of economic criteria. For example, El-Halwagi et al. (2013) developed a MILP model to consider both cost and safety issues of a biofuel supply chain covering feedstock production through the biofuel's end use, with the safety issue measured by potential fatalities associated with the biofuel supply chain. Results indicated that the economic and safety objectives contradicted each other over certain ranges.

You and Wang (2011) incorporated economic cost and GHG emissions to examine the optimal biofuel supply chain as a case study in Iowa, covering feedstock production in the field to the biofuel consumption, and found that efficient conversion technology was the key for commercialized LCB-derived biofuel production. You et al. (2012) conducted a county-level, multi-objective study on the LCB feedstocks supply chain in Illinois, concluding a tradeoff exists between the economic and environmental performance of the biofuel supply chain and the new jobs created were positively correlated with the economic cost of the supply chain. Bernardi et al. (2012) expanded the MILP model in Mas et al. (2010) to consider multiple objectives when optimizing the biofuel supply chain, and suggested that the NPV for biofuel production was positively related to both carbon emissions as well as water consumption.

Among the studies of LCB feedstock or biofuel supply chain, spatial data with different resolutions have been considered in different studies. For studies focusing non-spatial related objectives such as the selection of conversion technologies for biofuel production (e.g. Giarola et al. 2012), spatial data was infrequently addressed or neglected entirely. If a study's goals concerned land management-related perspectives such as land conversion of feedstock into LCB production (Perlack and Stokes, 2011) or the determination of location for biorefinery facility (Bowling et al., 2011), high resolution spatial data was usually incorporated (Marvuglia et al., 2013).

The application of GIS on land management-related projects started in the 1970s (Steinitz et al., 1976) in related areas including waste management (Gorsevski et al. 2012), agricultural and forestry (Morari et al. 2004), and regional planning (Ward et al. 2003). The major benefit of involving GIS into land use management has been its capability to perform an integrated analysis of spatial and attribute data (Couclelis, 1991). Besides, GIS tools have helped in multi-criterion analysis to display, manipulate, and evaluate various feasible alternatives during land use decision problems (Malczewski, 2006).

Integrating GIS with mathematical programming in the LCB supply chain design has occurred since the early 1990s (e.g. Graham et al., 1996a). For example, Dunnett et al. (2008) developed a MILP model which simultaneously determined the optimal design and operation schedules for a biomass-to-heat supply chain with cost minimization as an objective. The study area was decomposed into 25 homogeneous regions. Potential options for conversion technology, system scale, and supply/demand distribution were explored. The resulted indicated that the cost of biofuel production could be significantly reduced by increasing economies of scales and high-yield energy crops. Wu et al. (2010) assessed the feasibility of woody biomass based ethanol production in Central Appalachia with NPV maximization as the objective. By considering biomass availability, bale type, logistics, price, project financing and taxes, an optimal site for biofuel plant was located in West Virginia with an NPV of $68.11 to $84.51 million for a 20-year plant life.

2.2 Switchgrass Supply Chain Cost and GHG Emissions

Operations in the switchgrass supply chain related to both economic cost and GHG emissions are important elements in the optimization models. The economic cost of a switchgrass supply chain is influenced by the costs of fuel, materials, machinery and labor required for switchgrass production, harvest, storage and transportation. The conversion of other cropland into switchgrass also has an opportunity cost. The foregone profit from the previous production activity must be considered in the decision of land conversion to switchgrass production. Furthermore, GHG emissions emanate from activities related to land conversion, fuel combustion directly associated with the switchgrass supply chain and indirectly from the production of agricultural materials and machinery used in switchgrass production.

Among all these operations and procedures, several factors have been commonly discussed as potentially significantly affecting the economic cost or GHG emissions of the switchgrass supply chain.

Previous studies found that the cost of the switchgrass supply chain is affected by land use change, switchgrass harvest and storage technologies, and the associated feedstock supply region density. Since land for switchgrass is converted from other cropland or hay and pasture land, an opportunity cost needs to be considered in the breakeven price or payment to farmers to cover production expenses and provide the same net return compared with previous crops (James et al., 2010). The breakeven price differs among land with different profitability and crops. Mooney et al. (2009) studied the breakeven price based on a multi-location experiment in Tennessee, finding that yield, nitrogen fertilizer price, and fuel price influenced the breakeven price, ranging from $46 per Mg in the well-drained upland to $69 per Mg in the poorly drained flood plain in Tennessee. A similar study was conducted by Bangsund et al. (2008) to examine the breakeven price for switchgrass in south central North Dakota. Their study indicated that the breakeven price for switchgrass varied from $47 per Mg in low productivity soils to $76 per Mg in highly productivity soils when considering the profitability of previous crops.

Harvest and storage technology is also cited as major impact factors affecting supply cost. For example, the bale system used for the harvest and storage of switchgrass influences the cost of harvest, storage, and transportation. Hess et al. (2007) studied the economic competitiveness of LCB-based biofuel. The results indicated that 35-50% of biofuel production cost was from feedstock cost. In the study of the two conventional bale types, square and round, square bales have a larger throughput capacity than round balers, making them more cost-attractive during harvest, handling, and storage (Thorsell et al., 2004; English et al., 2008). However, round bales benefit from a lower dry matter loss (DML) rate during storage (Mooney et al., 2012). DML during storage influences cost in two ways: First, the DML is differentiated among different bale types and protection options. Cundiff and Marsh (1996) simulated the harvest cost for large round bales vs. large square bales. The results indicated that the harvest cost for round bales was $52.05/Mg while the cost for square bales was $37.6/Mg. Additionally, the storage period also influenced the feedstock loss rate. For example, Mooney et al. (2012) analyzed the optimal bale type with profit maximization among different bale systems, protection options, and storage period and found that the least cost solution considering harvest, storage, and transportation costs was via square bales stored with tarp covers on wood pallets. Round bales would not be optimal unless the price of switchgrass reached about $100 per Mg and the storage time reached 180 days. Besides these two conventional bale types, some studies had examined different preprocessing technologies such as dry chopping and wet chopping to lower the economic cost (Kumar and Sokhansanj, 2007).

The location of the biorefinery and the density of the supply region influence the transportation cost of the switchgrass supply chain. Yu et al. (2013) estimated the plant-gate cost of using two separate energy crops, i.e., switchgrass and energy sorghum, as the feedstocks for biofuel production. Given a fixed demand from the biorefinery, the results indicated the transportation cost would increase with a larger feedstock supply region and lower feedstock density for both feedstocks. Various transportation methods have also been examined. For instance, Kumar and Sokhansanj (2007) examined three transport options, i.e. bale transport, grind transport and chop transport, the results indicating that bale tranport had the lowest cost of $21.19/Mg, followed by grind transport with $23.19/Mg and chop transport with $25.32/Mg.

Two major sources of GHG emissions from the switchgrass supply chain are 1) land use change, and 2) energy consumption from switchgrass production, harvest, storage, transportation, and the production of seed, fertilizer, herbicide and machinery (Ney and Schnoor, 2002). Type of land converted to switchgrass production (e.g. Qin et al. 2011), harvest and storage technologies adopted (Kumar and Sokhansanj, 2007), and the feedstock supply region road network and topography (Yu et al. 2013) also influenced the GHG emissions from the switchgrass supply chain.

Different land types such as traditional crop (e.g. corn, soybean, and wheat), grassland, and switchgrass had different carbon sequestration rates. A proper assessment of the net CO_2 emissions from land use change should be the difference between carbon sequestration before and after the land use change (Adler et al., 2007). Particularly, Qin et al. (2011) examined the soil CO_2 emissions from the conversion of three major crops (i.e., corn, wheat and cotton) to switchgrass. The output indicated that the conversion from different crops into switchgrass production led to different soil CO_2 emissions. A recent study of Kwon et al. (2013) studied the potential of converting cropland and hay and pasture land into switchgrass production in the U.S. based on the CENTURY model, a plant-soil nutrient cycling model which simulates carbon and nutrient dynamics for different types of land. The output indicated that the conversion of cropland, hay and pasture land, conservation land and forest to switchgrass production led to different soil CO_2 emission factors. Moreover, the CO_2 emission factor varied among different states in the U.S. due to different soil properties and harvest schedules. For Tennessee, the conversion of cropland to switchgrass led to net GHG sequestration but the conversion of hay and pasture land to switchgrass led to net GHG emissions.

Another source of GHG emissions, N_2O emissions from switchgrass production is owed to the denitrification and partial denitrification process of applying fertilizer (Ney and Schnoor, 2002). In some studies, N_2O emissions have been regarded as the largest source of GHG emissions in the switchgrass supply chain (Adler et al., 2007, Crutzen et al., 2008). Moreover, the cattle located on hay and pasture land might have to be relocated if the hay and pasture land is converted into switchgrass production, possibility leading to GHG emission changes since cattle are a major contributor to CH_4 emissions based on the report of the Intergovernmental Panel on Climate Change (IPCC, 2006).

Besides land use change, the annual GHG emissions from switchgrass production and harvest varied along with different harvest and storage technologies such as different baling systems. Kumar and Sokhansanj (2007) indicated that the baling technology played an important role in determining the GHG emissions from switchgrass supply chain. They found that the GHG emissions from round bales were about 17% higher than the square bales. Different DML rates during storage served as another impact factor on GHG emissions, though less discussed. DML led to GHG emissions in two ways: First, due to DML during storage, more feedstock needs to be produced and this magnifies the GHG emissions generated. According to Emery and Mosier (2012), the increased feedstock production due to storage loss might increase GHG emissions by 5-53% for outdoor storage. In addition, the lost switchgrass goes through aerobic and anaerobic decomposition processes leading to CO_2 and CH_4 emissions (Mann and Spath, 2001). Qin et al. (2006) examination found that about 108 CO_2e gram of GHG were emitted due to dry matter degradation per Mg of switchgrass produced for co-firing for electricity.

GHG emissions generated from LCB feedstock transportation are directly linked to the mode of transport (Mahmudi and Flynn, 2006) and transport distance (Thornley, 2008). As for switchgrass supply chain, the density of feedstock supply region also affects the GHG emissions. Yu et al. (2013) analyzed the feedstock cost and transportation emissions of a switchgrass supply chain in Tennessee. The study output indicated that the topography of the road networks and the density of the feedstock supply region influenced the Vehicle Miles Traveled (VMT) during switchgrass transportation and consequent GHG emissions and air pollutants.

Chapter 3 Conceptual Framework

The process of locating the feedstock supply from various areas for a biorefinery to maintain its annual biofuel production of Q (gallons) is presented in a simplified conceptual model. The biorefinery is assumed to be built in an existing industrial park in the study area using switchgrass as the potential feedstock. Since no large-scale switchgrass production is currently available, a certain amount of agricultural land needs to be converted into switchgrass production to meet the biorefinery demand. The objective of the biorefinery is to develop an economically and environmentally sustainable feedstock supply chain that supplies the adequate feedstock.

Assuming the biorefinery has limited market power in the competitive transportation fuel market, the biorefinery is a price-taker of the market price P (\$/gallon). The profit of the biorefinery, π (\$), is defined in equation (1):

$$\pi = P \times Q - TC(Q) \tag{1}$$

where TC (\$) is the total cost of the biorefinery. Since P is exogenous to the biorefinery in the competitive biofuel market and Q is a given capacity, the revenue of the biorefinery, i.e., $P \times Q$ is predetermined. Thus, in order to maximize profit, the biorefinery will minimize its total cost TC, which consists of three parts: the capital cost of the biorefinery (C_C), the cost of operations during biofuel production (C_O), and the feedstock cost (C_F) (see equation (2)).

$$\text{min. } TC(Q) = C_C(Q) + C_O(Q) + C_F(Q) \tag{2}$$

Assuming the technology used for biofuel production and the capacity of the biorefinery are given (i.e. C_C and C_O are predetermined), the biorefinery minimizes feedstock cost for the economic sustainability target.

$$\text{min. } C_F(Q) \tag{3}$$

With no market price for switchgrass available, the feedstock cost at biorefinery gate including the cost of switchgrass production, harvest, storage and transportation as well as the opportunity cost for land conversion need to be considered. In contrast to the capital cost C_C and operation cost C_O, the feedstock cost C_F is heavily affected by spatial conditions such as the availability of feedstock and the road network for feedstock transportation (Noon et al., 2002). Thus, the feedstock cost could vary considerably depending on the location of the feedstock supply even though the biorefinery demand is fixed given the annual capacity of Q.

The feedstock supply chain is not only a source of cost but also GHG emissions. Previous studies indicated that spatial factors such as type of land use change can affect the GHG emissions generated from the switchgrass supply chain (E_F) (Kwon et al. 2013). Thus, the level of GHG emissions from the feedstock supply chain is also spatially dependent. Also, the operations in the feedstock supply chain, such as the production, collection, storage and transportation of feedstock, will also generate GHG emissions. Thus, considering both economic and environmental performance in the feedstock supply chain, the objective of this study is to minimize both the cost and GHG emissions associated with the feedstock supply chain in equation (4).

$$\min.\ (C_F(Q), E_F(Q)) \tag{4}$$

Given the conversion rate of ϑ (gallon/ton) for switchgrass-based biofuel, the total demand of switchgrass from the biorefinery, X (Mg), is showed in equation (5)

$$X = \frac{Q}{\vartheta} \tag{5}$$

To specify the spatial heterogeneity, the potential feedstock supply region for the biorefinery is decomposed into *n* small crop zones of identical area (e.g., 5 square miles). The acreage of switchgrass produced in each crop zone is defined as A_i (acre), and the yield of switchgrass y_i

(Mg/acre) also varies among different crop zones. The amount of switchgrass produced in each crop zone X_i (Mg) is then shown in equation (6).

$$X_i = A_i \times y_i \tag{6}$$

Assuming there is no DML during the switchgrass supply chain, the total amount of switchgrass produced from the crop zones is equal to the demand from the biorefinery in equation (7).

$$\sum_{i=1}^{n} X_i = \sum_{i=1}^{n} y_i \times A_i = \frac{Q}{\vartheta} \tag{7}$$

The conversion of hay and pasture land or cropland into switchgrass varies in terms of opportunity cost and GHG emission factors. Hay and pasture land has a lower profitability than cropland, so the cost of converting one acre of hay and pasture land is less than the cost of converting one acre of cropland. On the other hand, hay and pasture land has a higher carbon sequestration rate than cropland, so more GHG emissions are generated if hay and pasture land is converted compared with traditional cropland. To differentiate the sources of land conversion, the acres of hay and pasture land converted into switchgrass in each crop zone are defined as ${A_i}^{hay}$, and the acres of cropland are defined as ${A_i}^{crop}$ with the following relationship maintained.

$$A_i = {A_i}^{hay} + {A_i}^{crop} \tag{8}$$

In equation (9), r_i is defined as the ratio of hay and pasture land converted to the total acres of land converted in crop zone i.

$$r_i = \frac{{A_i}^{hay}}{A_i} \tag{9}$$

Considering the aggregated hay and pasture land converted to switchgrass in all crop zones for the biorefinery, the aggregated regional hay and pasture land ratio R (R$\in$ $[0,1]$) can be defined in equation (10):

$$R = \frac{\sum_i^n A_i \times r_i}{\sum_i^n A_i} = \frac{\sum_i^n X_i \times r_i / y_i}{\sum_i^n A_i} \tag{10}$$

The cost and GHG emissions of the feedstock supply chain are not only affected by the type of land conversion (r_i) in each crop zone but also the acres of land converted into switchgrass production (A_i) and the yield of switchgrass (y_i). For example, if one crop zone, $i1$ is closer to the biorefinery than the another one, $i2$, delivering one unit of feedstock from crop zone $i1$ to the biorefinery has a lower cost and lower GHG emissions compared with crop zone $i2$. Moreover, if crop zone $i1$ has a higher yield per acre compared with crop zone $i2$, then the cost and GHG emissions from producing one unit of switchgrass in crop zone $i1$ will be lower than crop zone $i2$. Therefore, the feedstock cost and GHG emissions are a function of these three factors:

$$C_F = C_F(A_1, A_2, \ldots, A_n;\ y_1, y_2, \ldots, y_n;\ r_1, r_2, \ldots, r_n) \tag{11}$$

$$E_F = E_F(A_1, A_2, \ldots, A_n;\ y_1, y_2, \ldots, y_n;\ r_1, r_2, \ldots, r_n) \tag{12}$$

Since R is also the function of A_i, y_i and r_i, the cost (C_F) and GHG emissions (E_F) from the switchgrass supply chain are functions of R with the given capacity Q and the consequent total feedstock demand X (see equation (5)) by aggregating the spatial dimension i.

$$C_F = C_F(R|Q) \tag{13}$$

$$E_F = E_F(R|Q) \tag{14}$$

Fig. 1 shows the relationship between the cost (C_F), GHG emissions (E_F) and the regional hay and pasture land ratio (R) in the feedstock supply chain. Given the demand of feedstock from the biorefinery (X), when R increases, more hay and pasture land is converted, and the total feedstock cost is then lowered. This is driven by the lower opportunity cost of switchgrass production from converting the less profitable hay and pasture land. Thus, on the surface of the feedstock cost and the hay and pasture land ratio (C_F-R) in Fig. 1, a negative relationship is presented (i.e. $\frac{dC_F}{dR} < 0$). When the hay and pasture land ratio increases from R1 to R2 and R3, the corresponding total feedstock cost reduces from c1 to c2 and eventually c3 (see points B'', O'' and A'' in the C_F-R surface, Fig. 1).

In contrast, with increasing R and the conversion of more hay and pasture land, the GHG emissions of the feedstock supply chain decreases since less carbon is sequestrated by switchgrass. As a result, a positive relationship is presented ($\frac{dE_F}{dR} > 0$) on the surface of the GHG emissions and the hay and pasture ratio surface (E_F-R) (Fig. 1). When the hay and pasture ratio increases from R1 to R2 and R3, more GHG emissions increase from e1 to e2 and e3 (see points B', O' and A' in the E_F-R surface, Fig. 1).

As in Fig. 1, by changing the hay and pasture ratio from R1 to R2 and R3, the corresponding cost and GHG emissions can be determined in the C_F-R surface (presented by points B'', O'' and A'') and E_F-R surface (presented by points B', O' and A'), respectively. As a result, a series of points can also be generated in the surface of the feedstock cost and GHG emissions (C_F-E_F), i.e., points A, O, and B. From point A to O and B, the feedstock cost increases from c3 to c2 and c1, while the GHG emissions decreases from e3 to e2 and e1. This indicates a tradeoff relationship between cost and GHG emissions in the feedstock supply chain ($\frac{dC_F}{dE_F} < 0$).

While the demand of feedstock from the biorefinery (X) is pre-determined, the tradeoff relationship between cost and GHG emissions from the feedstock supply chain results from the change of regional hay and pasture land ratio, R. As shown in equation (10), any given level of R represents specific combinations of crop zones with associated A_i, y_i, and r_i. To achieve higher economic performance in the feedstock supply chain, the crop zones with more hay and pasture land (e.g. east and middle Tennessee), higher switchgrass yield, and biorefinery proximity are preferred. On the other hand, crop zones with more traditional crop land (e.g. west Tennessee), higher switchgrass yield, and biorefinery proximity are chosen to mitigate GHG emissions in the feedstock supply chain. A balance of both objectives in the feedstock supply chain can be optimized through management of the tradeoff relationship (see Fig. 1) via the selection of crop zones.

Chapter 4 Methods and Data

4.1 The Case

The location of the biorefinery, a 50 million gallon facility, was assumed to be in Tennessee using technology that would convert a ton of switchgrass into 76 gallons of biofuel (Wang et al., 1999). Given the conversion rate, the monthly feedstock demand from the biorefinery required about 55 thousand tons of switchgrass. Switchgrass was assumed to be harvested annually from November to February under the available working hours in each month that were determined based on historical weather records. Switchgrass was assumed to be harvested, packaged in large 4×4×8 foot rectangular (square) bales and stored at the edge of the field (Mooney et al., 2012). Semi-truck trailers were used for switchgrass transportation from field to the biorefinery. The maximum distance from field to biorefinery plant was set to 75 miles to reduce solution time. A fixed DML rate (2%) was considered during switchgrass transportation (Kumar and Sokhansanj, 2007). The summary of the assumptions is given in Table 1.

4.2 Analytical Procedures

In this study, an augmented ε-constraint method was used to derive the tradeoff relationship between the two objectives considered, i.e., cost and GHG emissions. With the augmented ε-constraint method, one objective was optimized using the other objective as constraint (Mavrotas, 2009). According to Mavrotas (2009), solutions generated from the augmented ε-constraint method determined the tradeoffs of the two objectives considered, revealing how the performance of one objective changes with different performances of the other objective. In this study, the feedstock supply chain cost was minimized while a certain GHG emission level needed to be satisfied (as in equations (15)-(16)).

$$\text{min. } (C_F - \varepsilon \times \frac{s}{r}) \quad (15)$$

$$s.t.\ E_F + s = e \quad (16)$$

where C_F is the cost (\$), ε is a small number (in this study ε was set to be 10^{-3}), s is the non-negative slack variable, r is the range of the GHG emissions objective, E_F represents GHG emissions (CO_2e kg), and e is the constraint applied to the emission target from e_0 to e_n ($e \in [e_0, e_n]$, CO_2e kg). The slack variable is added in the objective function (16) with lower priority to assure that the program would choose the most efficient when several solutions have the same level of cost with differing GHG emissions (even if they were all lower than e).

Fig. 2 shows how the single-location tradeoff curve for biorefinery A with a given capacity (50 million gallons per year in this study) was generated by applying a series of GHG emission constraints from e_0 to e_n. Take point A^D in Fig. 2 as an example, by applying a specific GHG emission constraint e_d between e_0 and e_n, the economic cost c_d is determined with cost minimization, which gives one solution point for the ε-constraint method, i.e. A^D with (e_d, c_d). A prerequisite of using the ε-constraint method is to determine the range of the emission constraints, i.e. $[e_0, e_n]$, imposed on the GHG emission objective. To determine the minimum value e_0, a single-objective optimization to minimize GHG emissions is conducted as showed in equations (17)-(18).

$$\text{min. } E_F \quad (17)$$

$$s.t. \quad Q \quad (18)$$

The associated cost under the GHG emissions minimization is then post-calculated. This solution for cost and GHG emissions is depicted as point A^E. Since there is a tradeoff relationship between the two objectives, GHG emissions from the switchgrass supply chain increase with the reduction in cost. The maximum value e_n can be determined with a single-objective optimization to minimize the cost as showed in equations (19)-(20).

$$\min.\ C_F \tag{19}$$

$$s.t.\quad Q \tag{20}$$

Similarly, the determination of associated GHG emissions, e_n, is also an *ex-post* estimate. Point A^C in Fig. 2 represents such solution for cost and GHG emissions.

In practice, given a location for the potential biorefinery, optimization described in equations (17)-(18) is conducted to generate its minimal GHG emissions (e_0). Similarly, optimization described in equations (19)-(20) is conducted to generate its maximal GHG emissions (e_n). The (n+1) emission constraints from e_0 to e_n break down the range of $[e_0, e_n]$ into n equidistant parts. The ε-constraint method described in equations (15)-(16) is then conducted applying a series of emissions constraints from e_0 to e_n to generate the solutions points to generate the single-location tradeoff curve for the biorefinery A (Fig. 2).

On the tradeoff curve in Fig. 2, the relative changes of cost and GHG emissions show the imputed cost of reducing GHG emissions. For example, from solution point A^C to A^D, the imputed cost to reduce (e_0-e_d) CO_2e Mg of GHG emissions is \$(c_d-c_0), i.e. $\frac{c_d - c_0}{e_0 - e_d}$ (\$/CO_2e Mg), which is the absolute value of the slope of A^DA^C. Similarly, the imputed cost of reducing GHG emissions from A^D to A^E is $\frac{c_n - c_d}{e_d - e_n}$ (\$/CO_2e Mg). The imputed cost for GHG emission reduction changes along the tradeoff curve as the slope differs. As in Fig. 2, the absolute value of the slope of (A^D, A^C) is less than the one with (A^E, A^D), indicating that the imputed cost to reduce one unit of GHG emissions is higher when the solution point is between (A^E, A^D) rather than (A^D, A^C). Considerable GHG emissions could be reduced when increasing the cost between (A^D, A^C); however the cost for GHG emissions reduction in the range of (A^E, A^D) is much higher.

Since there are many eligible biorefinery locations in the study area (defined as the biorefinery candidates), multiple single-location tradeoff curves are generated and used to determine the regional tradeoff curve as shown in Fig. 3. Each dashed line represents a single-location tradeoff curve of a particular biorefinery candidate. For example, the green dashed line, blue dashed line, and purple dashed line represent the tradeoff curves for potential biorefinery locations A, B, and O, respectively. The red solid line represents the envelope of all the single-location tradeoff curves and is defined as the *regional tradeoff curve*. Every point on the regional tradeoff curve is not outperformed by any other points considering both cost and GHG emissions. The points above the curve are suboptimal solutions whose cost and GHG emissions could be reduced by the selection of different crop zones.

Among the four biorefineries included in Fig. 3, the biorefinery A has the minimal cost while biorefinery B has the minimal GHG emissions. Thus, the tradeoff curve for biorefinery candidate A shares the same point (A^C) at the cost minimal end of the regional tradeoff curve. Similarly, the biorefinery candidate B shares the same point (B^E) at the GHG emission minimal end of the regional tradeoff curve. Thus, the biorefinery candidate with the minimal potential cost (e.g. biorefinery A in Fig. 3) is defined as the *regional cost-minimal biorefinery candidate*. The biorefinery with the minimal potential GHG emissions (e.g. biorefinery B in Fig. 3) is defined as the *regional GHG emission-minimal biorefinery candidate*. Point A^C represents the solution point through the optimization process in equations (20)-(21) for the regional cost-minimal biorefinery candidate A. Similarly, point B^E represents the solution point from equations (18)-(19) for the regional GHG emission-minimal biorefinery candidate B.

The solution point A^C has the minimal potential cost achieved in the study area and the associated GHG emissions. Along with the regional tradeoff curve, an alternative solution point (the point O^I in Fig. 3) is determined by allowing 10% increases in the cost at solution point A^C. Point O^I is defined as an alternative optimal solution point and the associated biorefinery O is defined as the *regional alternative optimal biorefinery candidate*. The differences in GHG emissions between points A^C and point O^I show the reduction in GHG emissions by increasing 10% in the cost of LCB feedstock supply chain compared with the regional cost-minimal point A^C. A similar concept of the imputed cost to reduce GHG emissions introduced in Fig. 2 exists in the regional tradeoff curve as well. For example, the imputed cost of moving from point A^C to O^I is $\frac{1.1 \times C_A - C_A}{E_A - E_O}$ (\$/CO_2e Mg).

A multi-objective model is developed to evaluate the potential tradeoff between the two objectives, i.e. cost minimization and GHG emissions minimization. The components used to calculate the economic cost and GHG emissions are summarized in Table 2. Through optimizing the dual objectives, the model determines the following variables:

1. Location of the biorefinery and associated feedstock supply region,
2. Amount of land converted from different types of previous crop, and
3. Input use including energy consumption, fertilizer herbicide, seed and farm machinery usage.

4.3 Structure of Cost (C_F)

The cost of switchgrass at the biorefinery gate can be described using.

$$C_F = C_{opportunity} + C_{production} + C_{harvest} + C_{storage} + C_{transportation} \quad (21)$$

where C_F is the total economic cost (\$) of the switchgrass supply chain, and $C_{opportunity}$, $C_{production}$, $C_{harvest}$, $C_{storage}$, and $C_{transportation}$ are opportunity costs from land conversion, production cost, harvest cost, storage cost and transportation cost of switchgrass, respectively.

The breakeven price (BEP_{ipb}) is the minimal payment to farmers to convert a crop into switchgrass production (James et al., 2010). It is categorized into three components: the opportunity cost of land use change, the production cost of switchgrass, and the harvest cost of switchgrass. The opportunity cost ($C_{opportunity}$) for switchgrass production equals the profit of previous crop type as presented in equation (22). If cropland revenue is less than the county-level land rent, the land rent for crop and pasture is used instead.

$$C_{opportunity} = \begin{cases} \sum_{ipb}(\frac{Price_{ip} * Yield_{ip} - PC_{ip}}{Yield_i^{swi}} * XC_{ipb}) \text{ , if } (Price_{ip} * Yield_{ip} - LR_{ip}) \geq 0 \\ \sum_{ipb}(\frac{LR_{ip}}{Yield_i^{swi}} * XC_{ipb}) \text{ , } \quad \text{if } (Price_{ip} * Yield_{ip} - LR_{ip}) < 0 \end{cases} \tag{22}$$

The definition of the parameters and variables used in equation (22) and following equations are included in Table 3. The production cost for switchgrass production ($C_{production}$) in equation (23) include the establishment cost of the first year as well as an annual maintenance cost.

$$C_{production} = \sum_{ipb}(\frac{\text{Est+AM}}{Yield_i^{swi}} * XC_{ipb}) \tag{23}$$

The labor, fuel, and machinery costs for switchgrass harvest are taken into account in harvest cost (C_{harvest}). Harvest technologies such as bale type influenced the cost since different machineries with different fuel consumption rates were used (equation (24)).

$$C_{harvest} = \sum_{ipb}(\frac{\text{Sigma}_{ib}}{Yield_i^{swi}} \times XC_{ipb}) \tag{24}$$

Combining the cost components in equations (22)-(24), the breakeven-price of switchgrass is expressed in equation (25):

$$BEP_{ip} = \begin{cases} \frac{Price_{ip} * Yield_{ip} - PC_{ip} + Est + AM + \text{Sigma}_{ib}}{Yield_i^{swi}} \text{ , if } (Price_{ip} * Yield_{ip} - LR_{ip}) \geq 0 \\ \frac{LR_{ip} + Est + AM + \text{Sigma}_{ib}}{Yield_i^{swi}} \text{ , } \quad \text{if } (Price_{ip} * Yield_{ip} - LR_{ip}) < 0 \end{cases} \tag{25}$$

Storage cost for switchgrass (γ_{ibt}) entails the cost of materials usage and the cost from equipment and labor completing storage operations such as bale stack and tarp. Semi-trailer trucks comprise switchgrass transportation. The sources for switchgrass transportation cost (θ_{ib}) include labor, energy consumption, and machinery maintenance during switchgrass loading/unloading and transportation. They are determined by the time consumed during each process. Loading/unloading time for square bale is adopted from the study of Duffy (2007), and it is assumed a the round bale consumed 10% more time than a square bale. Distance and speed determine the time consumption during transportation. The calculation of the storage cost and transportation cost are presented in equations (26) and (27), respectively.

$$C_{storage} = \sum_{mipbt} \gamma_{ibt} * NXS_{mipbt} \tag{26}$$

$$C_{transportation} = \sum_{ib} \theta_{ib} \times \frac{\sum_{mp} XTN_{mipb} + \sum_{mpt} XTO_{mipbt}}{1 - DMLT} \tag{27}$$

4.4 Structure of GHG Emissions (E_F)

The sources of GHG emissions of the switchgrass supply chain are land use change (E_{luc}), energy consumption from switchgrass production, storage harvest (E_{energy}), transportation ($E_{transportation}$), and the production of seed, fertilizer, herbicide and machinery (E_{ind}). Equations to calculate the GHG emissions from these sources are given in (28)-(32), and the definitions for parameters and subscripts are also in Table 3. The sources of GHG emission parameters in the equations (28)-(32) are introduced in section 5.4.3.

$$E_F = E_{luc} + E_{energy} + E_{transportation} + E_{ind} \tag{28}$$

$$E_{luc} = \sum_{mipb} \left(lucE^{co2}{}_p + lucE^{n2o}{}_p \right) * AH_{mipb} \tag{29}$$

$$E_{energy} = \sum_{mipb} storE * XH_{mipb} + \sum_{mipb} (proE + harE_b) * AH_{mipb} \tag{30}$$

$$E_{transportation} = \sum_{mib} transE_{mip} * \frac{\sum_p XTN_{mipb} + \sum_{pt} XTO_{mipbt}}{loadwt_{mib} * (1 - DMLT)} \tag{31}$$

$$E_{ind} = \sum_{mipb} (fertE + herbE + seedE) * AH_{mipb} + \sum_{mb} Numb_{mb}{}^k * mac\mathrm{hE}^k \tag{32}$$

Two kinds of GHG emissions from land use change are estimated in equation (29), i.e., CO_2 ($lucE^{co2}{}_p$) and N_2O ($lucE^{n2o}{}_p$). Both CO_2 and N_2O emissions from land use change depend on different among different types of land p converted into switchgrass production. In equation (30), the energy consumption from switchgrass production ($proE$), harvest ($harE_b$), and storage ($storE$) are considered. GHG emissions from energy consumption for production and harvest are based on per acre of switchgrass produced and GHG emissions from storage were based on per Mg of switchgrass stored. In equation (31), GHG emissions from switchgrass transportation are calculated with the emission factor ($transE_{mip}$) specifying the route from the supply region to the biorefinery. Moreover, indirect sources of GHG emissions include the production of machinery, fertilizer, herbicide and seed (as depicted in equation (32)).

4.5 Structure of Constraints

Several constraints about feedstock availability and inventory flow need to be satisfied for the switchgrass supply chain. Switchgrass production is restricted by the available land and yield. Equation (33) limits the switchgrass land to be less than or equal to maximum amount potential land available. PAS_p (%) represents the percentage of land p that is allowed to be converted in to switchgrass production. Specifically, there is no limit on the percentage of cropland to be converted (i.e. $PAS_{crop} = 100\%$), and it is assumed that the biorefinery could not convert more than 50% of available hay and pasture land (i.e. $PAS_{hay} = 50\%$) to maintain the local cattle inventory. Equation (34) limits the amount of switchgrass produced to be less than or equal to the maximum potential amount. The definition of the parameters and variables in all equations in this section are also listed in Table 3.

$$\sum_b A_{ipb} \leq PAS_p \times aa_{ip} , \forall i, p \tag{33}$$

$$XC_{ipb} \leq Yield_i^{swi} \times A_{ipb} , \forall i, p, b \tag{34}$$

Equations (35)-(38) are related to switchgrass harvest. Equation (35) indicates that no more switchgrass was harvested than produced. Equation (36) indicates that the amount of switchgrass harvested each month is constrained by the available working hours in each month ($rateava_m$). Equation (37) limits the harvest season of switchgrass from November to February. Equation (38) calculates machinery usage during switchgrass harvest.

$$XC_{ipb} - \sum_m XH_{mipb} \geq 0, \ \ \forall\, i, p, b \tag{35}$$

$$\sum_{i,p,b} XH_{mipb} = \frac{CapUnit}{\lambda} \times \ rateava_m, Dec \ \leq m \leq Feb \,\&\, \forall\, m \tag{36}$$

$$XH_{mipb} = 0 \ , \ \ March \ \leq m \leq Oct\ \forall\, m, i, p, b \tag{37}$$

$$Numb_{mb}{}^{k} \times avehour_m - \sum_{i,p} (mtb_{ib}{}^{k} \times AH_{mipb}) \geq 0 \ , \ \ \forall\, m, b \tag{38}$$

Equation (39) shows that the newly stored switchgrass in each month m equals the amount of switchgrass harvested deducting the amount of switchgrass delivered to the biorefinery directly. Equations (40) to (43) determine the accumulative switchgrass storage. During harvest season, accumulative switchgrass storage equals the amount stored in previous month plus the newly stored amount as presented in equation (40). During off-harvest season, accumulative switchgrass storage equals the amount stored in the previous month minus the amount of switchgrass delivered to biorefinery in the current month, as presented in equation (41). Equation (42) indicates that there is no switchgrass carryover between crop years. Equation (43) indicates that the switchgrass delivered to biorefinery each month meets the demand.

$$\sum_t^2 NXS_{mipbt} = XH_{mib} - \frac{XTN_{mipb}}{1-DMLT}, \ \ Nov \ \leq m \leq Feb \ \&\, \forall\, m, i, p, b \tag{39}$$

$$XS_{(m+1)ipbt} = (1 - DMLS_{mbt}) \times XS_{mipbt} + \ NXS_{(m+1)ipbt} \ , \ \ \ Nov \ \leq m \leq Feb \,\&\, \forall\, m, i, p, b, t \tag{40}$$

$$XS_{(m+1)ipbt} = (1 - DMLS_{mbt}) \times XS_{mipbt} - \ \frac{XTO_{(m+1)ipbt}}{1-DMLT} \ , Mar \leq m \leq Oct\ \forall\, m, i, p, b, t \tag{41}$$

$$XS_{mipbt} = 0\ ,\ m = Oct\ \&\ \forall\ m, i, p, b, t \tag{42}$$

$$\lambda(\sum_{i,p,b} XTN_{mipb} + \sum_{i,p,b,t} XTO_{mipbt}) = Dd_m\ ,\ \forall\ m \tag{43}$$

4.6 Data

4.6.1 GIS Data

The detailed GIS data used in this study was obtained from a GIS model, the Biofuel Facility Location Analysis Modeling Endeavor (BioFLAME) (Wilson, 2009). More than 230 industrial parks in Tennessee were considered as potential candidates for biorefinery location in Tennessee based on the Tennessee Valley Authority. All of the industrial parks selected had sufficient access to water, power, and roads, as well as sufficient storage space. To determine the potential feedstock supply region, all the traditional cropland, e.g. corn, wheat, soybean, sorghum, cotton and hay, in Tennessee and within 50 miles of the state border was considered. Public land such as national parks was excluded from the study. All the potential land was decomposed into five square-mile hexagons (defined as crop zones) (Fig. 4). Additionally, a street level network was applied to generate the most accessible routes from each supply crop zone to the potential biorefinery with the following hierarchy: 1) primary/major roads, 2) secondary roads, 3) local and rural roads, and 4) other roads.

4.6.2 Data for Cost Estimation

To estimate the total cost the switchgrass supply chain, information about the opportunity cost from traditional crop cultivation and the cost from switchgrass production, harvest, storage and transportation needed to be gathered. The traditional crop yield was obtained from the SSURGO Database at the sub-county level (USDA, 2012). Acres in each crop zone for each crop type were derived from the Cropland Layer Database (USDA National Agricultural Statistics Service, 2011). The price of the traditional crops was the three-year average price i.e., 2010-12, obtained from the National Agricultural Statistics Service, USDA (2013a). The production cost for traditional crops was from the Agricultural Policy Analysis Center's Agricultural Budgeting System.

Potential switchgrass yield was obtained from the Oak Ridge Energy Crop County Level Database (Graham, et al. 1996b) (see Fig. 5). The production and harvest costs for switchgrass were taken from Larson, et al. (2010), and the budgets were developed by the University of Tennessee Department of Agricultural and Resource Economics (Gerloff, 2008).

For switchgrass establishment, two burndowns were conducted in the August of the previous year as well as in the early May for weed control. Fertilizer application and post establishment spray were also conducted afterwards (Switchgrass Budget, UT Extension). The energy, labor and maintenance costs for operating equipment and capital costs were considered based on the estimated cost factors compatible with the American Agricultural Economics Association Cost and Return Handbook (AAEA, 2010) and American Society of Agricultural Engineers Standards (ASAE, 2006). After amortization to each year, the cost parameter of establishment was $61.05 per acre. Annual maintenance of switchgrass (AM), including the application of fertilizer as well as herbicide, was $46.83 per acre.

Semi-trailer trucks were used for switchgrass transportation, and the assumed utilization was 16.01 Mg/load for square bales and 13.18 Mg/load for round bales (Wang et al. 2009). Main sources for switchgrass transportation cost were labor, energy consumption, and machinery maintenance during switchgrass loading/unloading and transportation as determined by the time consumed during each process. The loading/unloading time for square bales was adopted from the study of Duffy (2007) and it was assumed that the round bale consumed 10% more time than the square bale. The distance and speed determined time consumption during transportation. As discussed in 4.2, both the distance and average transportation speed were generated based on the most accessible route from a street level network.

4.6.3 Data for GHG Emission Estimation

To estimate the GHG emissions from the switchgrass supply chain, emission information for all the supply chain procedures needed to be gathered. The DAYCENT model, a daily time-step version of the CENTURY (Parton et al. 1994) biogeochemical model was adopted to simulate the soil CO_2 and N_2O emission factors due to the conversion of different types of land into switchgrass production. Factors such as soil property, crop type, and weather were included in the DAYCENT model (Schimel et al., 2001). Especially, the DAYCENT model has been found to be adequate for predicting the relative differences with changes in parameters (Chamberlain et al., 2011), making it useful for comparing different land use conversions.

To apply the DAYCENT model, weather and soil data in Tennessee were needed. The annual weather data for Tennessee was acquired from the DAYMET[1] model maintained by the Oak Ridge National Laboratory. The soil property data used in the DAYCENT were from U.S. Geological Survey.[2] Based on the soil property data which showed the clay, sand and silt percentage, the soil type was determined by the Soil Texture Triangle Hydraulic Properties Calculator (Saxton et al., 1986).

To calculate the difference in the soil carbon change by land use change, two cases were simulated and each of them had a time period of 60 years in the DAYCENT. In case 1, each of the major crops in Tennessee was planted and harvested for 60 years. In case 2, the same crop was planted and harvested for 30 years, and then this land was converted to produce switchgrass for the following 30 years. The DAYCENT was used to simulate the soil carbon content at the

---

[1] DAYMET model is available at: http://daymet.ornl.gov/custom_home
[2] The soil property data is available at : http://water.usgs.gov/GIS/metadata/usgswrd/XML/statsoil.xml

end of the period for each case. The difference in the soil carbon contents between these two cases was the soil CO_2 emissions/reduction due to changes in land use. Moreover, the DAYCENT also simulated the annual N_2O emissions from the switchgrass land.

The emission factors for soil CO_2 and N_2O emissions from the land conversion of crops in to switchgrass production are summarized in Fig. 6, which illustrates that the conversion of different crops into switchgrass led to different carbon change rates as well as N_2O emission rates. The conversion from conventional crops (such as corn, cotton, and soybean) to switchgrass led to net carbon sequestration since switchgrass is a perennial grass with a high carbon sequestration rate. However, the conversion from hay or pasture into switchgrass led to net carbon emission since hay is also perennial and sequestrated more carbon than switchgrass.

The Greenhouse Gases, Regulated Emissions, and Energy Use in Transportation (GREET) Model (Wang, 2010), which was developed and is maintained by the Argonne National Laboratory, provided the emission factors for all the three GHG emissions from machinery combustion during LCB harvest. According to the GREET model, one gallon of diesel consumed by the farming tractor led to 77,411 grams CO_2, 0.99 grams of N_2O and 0.63 grams of CH_4 emissions.

According to the switchgrass budget from UT Extension, all the farming equipment such as mowers, loaders, balers and rakes worked together with a tractor, making tractor the only source of energy consumption. The diesel consumption was calculated from the time used during each operation (hours/acre) times the fuel use (gallon/hour) of the tractor. Operations for square bale system used 19.78 gallon per acre for the whole supply chain, while operations for round bale system consumed 25.34 gallon per acre. Switchgrass harvest caused 405 CO_2e kg per acre annually using square bale technology and 519 CO_2e kg per acre annually for round bale system.

GHG emissions from energy consumption during switchgrass production and storage were less: about 33 CO_2e kg and 2 CO_2e kg GHG were emitted from production and storage, respectively.

GHG emissions from switchgrass transportation also resulted from semi-truck diesel consumption. In addition to travel distance, a typical factor used to estimate transportation emission, more factors needed to be considered. For example, emissions from truck emissions vary given different seasons, speeds, and the slopes of road. In order to take all these factors into consideration, the Motor Vehicle Emissions Simulator (MOVES) was used to estimate the truck emissions of switchgrass from field to biorefinery plant gate. Developed by Office of Transportation and Air Quality (OTAQ) of EPA, MOVES was used in different regions and levels to consider factors such as travel speed, season, road slope, etc. The version used in this study was MOVES2010a[3]. Applying the MOVES model, the GHG emissions for each optimal route linking between supply crop zones and potential biorefinery sites were calculated.

Indirect emissions refer to GHG emitted during the production of agricultural machinery, fertilizer, herbicide, and seed. The machinery used during switchgrass production and harvest include tractors, mowers, balers, loaders, and rakes. Energy, steel, and tire consumption during machine production lead to GHG emissions. Emission factors for steel and tire were also adopted from GREET model (Wang, 2010). The weight of different machinery was based on the "Official Guide: Tractor and Farm Equipment" (Spring 2010) and machinery manufacturer websites such as John Deere[4]. Fertilizer production emission factors were also adopted from the GREET model, while the application rate was adopted from Switchgrass Budget database (Gerloff, 2008). According to the Switchgrass Budget database, three kinds of herbicide were used for switchgrass: Roundup, Cimarron, and grass herbicide. The production GHG emissions

[3] MOVES2010a is available at: http://www.epa.gov/otaq/models/moves/.
[4] Website for John Deere: http://www.deere.com/wps/dcom/en_US/regional_home.page

for these three herbicides were based on the work of Nelson et al. (2009). Emission parameters for switchgrass seed production were adopted from Wilson et al. (2011). The summary of the emission factors is presented in Table 4.

4.7 Sensitivity Analysis

Two scenarios were conducted to evaluate the impacts of different GHG emissions parameters on the initial optimization output (referred to as the baseline). The first scenario assessed the GHG emissions from DML decomposition, while the second scenario considered the alternative option when relocating the cattle from the hay and pasture land converted to switchgrass production. A comparison between the baseline and the two sensitivity analyses are listed in Table 1.

4.7.1 Scenario 1: Emission from DML

The study of Emery and Mosier (2012) indicated that DML during storage and transportation led to not only more switchgrass production and related GHG emissions but also to direct GHG emissions from the DML decomposition. According to Mann and Spath (2001), the DML occurred through anaerobic as well as aerobic decomposition, causing both CO_2 and CH_4 emissions. Qin et al. (2006) followed their method and concluded that the decomposition of one Mg of switchgrass led to 1,278 kg of CO_2 and 62 kg of CH_4. Considering global warming potential, one Mg of DML led to 2,820 CO_2e kg of GHG emissions.

In the baseline, the GHG emissions from producing additional switchgrass due to DML were included; however, the GHG emissions from DML decomposition were not considered. In the sensitivity analysis, an additional component was added in the GHG emission objective function (equation (28)) to consider the GHG emissions from DML decomposition. This part of GHG emissions is represented in equation (42):

$$E_{loss} = \sum_{mibp}(XH_{mipb} - XTN_{mipb} - XTO_{mipb}) * lossE \quad (44)$$

As defined in Table 3, the *lossE* is an emission factor (CO_2e kg/Mg) for GHG emissions from DML decomposition. Since the harvest and storage technologies have a significant impact on the DML rate, three potential harvest and storage technologies were examined in this scenario. The first analyzed technology was the square bale with tarp and pallet, which was the technology adopted in the baseline. The second evaluated technology was the round bale without tarp or pallet. Since the DML rate was lower with the round bale (Mooney et al., 2012), the output showed how the DML rate affected the GHG emission level of the switchgrass supply chain. Finally, the third analyzed technology was assumed to be an improved square bale that ultimately controlled the storage DML (i.e. DML during storage was reduced to zero).

4.7.2 Scenario 2: Emission from Cattle Removal

If hay or pasture land was converted into switchgrass for biofuel, the cattle on the hay and pasture land were also relocated. In the baseline, it was assumed that the reduction in hay and pasture led to increased density of cattle on the remaining hay and pasture land in the study area and the total inventory of cattle remained unchanged. However, in scenario 2, the cattle inventory was considered to be migrated to other areas and consequent GHG emission change were then analyzed.

According to the 2006 IPCC Guidelines for National Greenhouse Gas Inventories, the CH_4 emission from dairy cattle including both enteric fermentation and manure management was 186 kg CH_4 per head per year while the emission factor for beef cattle was 54 kg CH_4 per head per year (IPCC, 2006). In this scenario, the GHG emissions from cattle migrating to other areas were also considered in the GHG emission objective function. The new equations (45)-(46) were used instead of the previous equation (29).

$$E_{cattle} = \sum_{mibp} AH_{mipb}{}^{hay\&pasture} * \tau_i * cattleE \tag{45}$$

$$E_{luc} = \sum_{mipb}\left(lucE^{co2}{}_p + lucE^{n2o}{}_p\right) \times AH_{mipb} - E_{cattle} \tag{46}$$

where E_{cattle} is the change of GHG emissions due to the relocation of cattle and τ_i is the density of cattle (head/acre) for each county in the study area (Fig. 7). The definitions of the parameters are presented in Table 3.

Two cases of cattle inventory migration were analyzed in this scenario. In the first case, 50% of the cattle inventory in the feedstock supply region were moved out of the study area, which implies that all cattle on the maximum allowable hay and pasture land (i.e. $PAS_{hay} = 50\%$) in the feedstock supply region in baseline were gone. Thus, the reductions in GHG emissions of all cattle on the pasture and hay land converting for switchgrass production in baseline were considered in the total GHG emissions estimation. In the second case, it was assumed that 25% of the cattle inventories were migrated. As a result, the reduction in the GHG emissions produced from half of the cattle population in the feedstock supply region were considered in the total GHG emissions estimation by setting $PAS_{hay} = 25\%$.

Chapter 5 Results and Discussion

5.1 Output for Baseline

The cost and GHG emission output of the regional cost-minimal solution point (A_0^C), regional GHG emission-minimal solution point (B_0^E), and the regional alternative optimal solution point (O_0^I) in Fig. 3 are summarized in Table 5. At the regional cost-minimal solution point A_0^C, the total cost of the switchgrass supply chain was nearly $46 million and the total GHG emissions were higher than 81,000 CO_2e Mg (see Table 5). Among the different sources for cost, switchgrass harvest was dominant, accounting for nearly 50% of the total cost. Switchgrass transportation and production made up 23% and 19% of the total cost, respectively. The opportunity cost and storage cost together contributed the remaining 10% of the total cost. Energy consumption, including switchgrass production, harvest and storage, was the major GHG emission source, contributing 45% of total GHG emissions. Emissions from transportation and indirect emission from the production of machinery and material accounted for 5% and 19% of the total emissions, respectively. GHG emissions from changes in land use, including the CO_2 and N_2O emissions from soil, contributed 31% of the total emissions (see Table 5). The biorefinery with the regional cost-minimal solution, A_0 (i.e. the regional cost-minimal biorefinery candidate) was located in Rutherford County, south of Nashville (see Fig. 8). The total acreage of switchgrass was 79,816 acres, extending to 406 crop zones and producing about 727,366 Mg of switchgrass in total. Nearly 98% of land was converted from hay and pasture, while only 2% of land was converted from cotton, soybean and wheat, with no land from corn converted (see Table 5).

At the regional GHG emission-minimal solution point B_0^E, the total cost of the switchgrass supply chain was $85 million, about 1.8 times higher compared with the regional cost-minimal solution point A_0^C. The total GHG emissions for B_0^E were about 29,000 CO_2e Mg, which was 36% of GHG emissions from the regional cost-minimal point A_0^E. Among the different sources of cost, opportunity cost contributed to nearly 50% of the total cost, followed by switchgrass harvest, which accounted for 26%. Both switchgrass transportation and production made up to 10% of the total cost, and storage made up to the remaining 4%. Energy consumption was the major source of GHG emission, producing more than 37,000 CO_2e Mg GHG. Together with switchgrass transportation and other indirect sources, the total GHG emissions reached 55,000 (37,115+1,757+16,037) CO_2e Mg. However, with solution point B_0^E land use change became a source of GHG emission sequestration. Land use change reduced about 26,000 Mg of CO_2 (see Table 5). The regional GHG emission-minimal biorefinery candidate B_0 was located in Obion County in northwest Tennessee (see Fig. 8). More than 80,000 acres of land were converted from 133 crop zones, and all the land was converted from traditional cropland, i.e. corn, cotton, and wheat (see Table 5).

At the regional alternative optimal solution point O_0^I, the cost was about \$51 million, 10% higher than the solution point A_0^C, while the GHG emissions were about 35,000 CO_2e Mg. Harvest was still dominant, accounting for 45% of the total cost. Cost from production and transportation made up 18% and 17% of the total cost, respectively. The opportunity cost from land conversion was around \$7.3 million, about 14% of the total cost. Storage accounted for 5% of the total cost. Energy consumption remained the major source of GHG emissions, producing nearly 38,000 CO_2e Mg GHG. Together with switchgrass transportation and other indirect sources, the total GHG emissions reached 56,000 (37,986+1,989+16,356) CO_2e Mg GHG. GHG emission reduction from land use change was about 21,000 CO_2e Mg. The location for the regional alternative optimal biorefinery candidate O_0 was in Haywood County in southwest

Tennessee (see Fig. 8). More than 82,000 acres of land were converted form 176 crop zones. About 7% of the land was converted from hay and pasture while the remaining land was converted from traditional crop land.

All the solution points, including the three discussed above (i.e. A_0^C, B_0^E, and O_0^I), are shown in Fig. 9. For each potential biorefinery candidates, four solution points were generated. Taking biorefinery candidate A_0 as an example: A_0^C represents the solution point with the optimization described in equations (19)-(20), and A_0^E represents the solution point with the optimization described in equations (17)-(18). Two other solution points (as depicted as the red dots in Fig. 8) were also generated with the ε-constraint method described in equations (15)-(16). Since there were 233 biorefinery candidates in the study area, Fig. 9 contains 932 (4×233) solution points.

Given all solution points shown in Fig. 9, the regional tradeoff curve for the baseline is presented as a solid blue curve in Fig. 10. The two dashed lines in Fig. 10 represent for the single-location tradeoff curves for the regional cost-minimal and regional GHG emission-minimal biorefinery candidates. As expected, the two single-location tradeoff curves were in the sub-optimal zone of the regional tradeoff curve. The right side of the regional tradeoff curve was flat, indicating the potential to reduce GHG emissions in the switchgrass supply chain by sacrificing relatively minor cost, i.e., the imputed cost for reducing GHG emissions was small. For example, from the regional cost-minimal solution point A_0^C to the alternative optimal solution point O_0^I, the cost of reducing 46,000 CO_2e Mg GHG emissions was \$4.6 million, which was about \$0.10/CO_2e kg. The left side of the tradeoff curve was relatively steep, indicating that the imputed cost for reducing GHG emissions was higher. For example, from the regional GHG emission-minimal solution point B_0^E to the alternative optimal solution point O_0^I, the cost of reducing 5,686 CO_2e Mg was $35 million, which was about $6.11/$CO_2$e kg.

The tradeoff relationship between cost and GHG emissions primarily resulted from the type of land conversion into switchgrass production. Fig. 11 showed the regional hay and pasture land ratio (R) and its influence on cost and GHG emissions for the three biorefinery candidates of the baseline. *R* for solution points B_0^E, O_0^I, and A_0^C was 0%, 7.4% and 98% respectively. The increase of the hay and pasture land ratio had a positive impact on the economic performance of the switchgrass supply chain; however, it resulted in more GHG emissions.

The type of land conversion affected the tradeoffs between cost and GHG emissions in two steps: First, different types of land conversion influenced opportunity cost as well as GHG emissions from soil. Cropland and hay and pasture land had different profitability and carbon sequestration rates. Cropland such as corn, soybeans and wheat had higher profit compared with hay and pasture land, making the conversion of traditional land more expensive in terms of opportunity cost than hay and pasture land. Therefore, the opportunity cost for the solution points of B_0^E, O_0^I, and A_0^C were $42.4 million, $7.3 million, and $1.6 million, respectively, when more hay and pasture land was converted (see Fig. 11 and Table 5). Also, different crops had different carbon sequestration rates. Hay and pasture had a higher carbon sequestration rate than switchgrass, making conversion to switchgrass production a net source of GHG emissions. Conversion of cropland had a lower carbon sequestration rate than switchgrass, making such changes in land use a net source of carbon sequestration. Thus, under cost minimization, more hay and pasture land would be converted but cropland would be converted when minimizing GHG emissions. The GHG emissions from land use change led to -25 million, -21 million, and 25 million CO_2e kg GHG emissions for solutions of B_0^E, O_0^I, and A_0^C, respectively, given the increasing amount of hay and pasture land converted (see Fig. 11 and Table 5). As a result, land use change was the leading cause of variation in the total GHG emissions.

Second, different types of land conversion affected the location of biorefinery and the density of the feedstock supply region since the availability of different land types and the switchgrass yield varied among different regions. As shown in Fig. 5, cropland in middle Tennessee had the highest yield per acre of land converted. Besides, there was also a great amount of hay and pasture land available in the region. These two were the primary reasons for locating the regional cost-minimal biorefinery candidate A_0 in Rutherford County, middle Tennessee. On the other hand, more cropland such as corn, cotton and wheat was available in the plain in west Tennessee. As a result, the regional GHG emission-minimal biorefinery candidate B_0 was sited in Obion County, west Tennessee. The regional alternative optimal biorefinery candidate O_0 was sited in Haywood County, west Tennessee since more than 90% of the supply region was also converted from cropland. The density of the supply region for the regional cost-minimal biorefinery candidate A_0 was lower than those associated with B_0 and O_0 since more crop zones were converted (Table 5 and Fig. 8). In middle Tennessee, the hay and pasture land was more scattered compared with the cropland in west Tennessee. As a result, the transportation-related cost and GHG emissions were also higher for biorefinery candidate A_0 compared with the biorefinery candidates B_0 and C_0 (see Table 5).

5.2 Output for Scenario 1: GHG Emissions from DML

The effects of considering the DML emissions on the estimated cost and GHG emissions from the switchgrass supply chain are presented in Tables 6-8. Table 6 summarizes the cost and GHG emissions output of the regional cost-minimal solution point (A_1^C), regional GHG emission-minimal solution point (B_1^E), and the alternative optimal solution point (O_1^I) with square bale system (Scenario 1-a). Tables 7 and 8 summarize the cost and GHG emissions for the three selected solution points, i.e., A_2^C, B_2^E, and O_2^I for round bales (Scenario 1-b) and A_3^C, B_3^E, and O_3^I with the square bale system, and no DML during storage (Scenario 1-c).

The different cost components for solution points A_1^C, B_1^E, and O_1^I in Scenario 1-a (see Table 6) remained the same compared with the three solution points A_0^C, B_0^E, and O_0^I in the baseline (see Table 5), respectively. The GHG emissions from the three solution points, on the other hand, were much higher compared with the baseline. GHG emissions from the DML were the key difference. Cost for A_2^C, B_2^E, and O_2^I from Scenario 1-b presented in Table 7 was higher than A_0^C, B_0^E, and C_0^I in the baseline. Though there was no storage cost for the round bale system in Scenario 1-b, the increasing harvest and transportation cost of switchgrass generated more total cost. The GHG emissions from Scenario 1-b were much higher compared with the baseline but lower than GHG emissions from Scenario 1-c. With square bales and no DML during storage, the cost for Scenario 1-c was the lowest among the baseline and Scenarios 1-a, 1-b, and 1-c. While its GHG emissions were still higher than baseline after considering the decomposition of DML from transportation, Scenario 1-c remained lower than both Scenarios 1-a and 1-b.

Fig. 12-14 shows the associated locations and feedstock supply regions for Scenarios 1-a, 1-b and 1-c, respectively. The regional cost-minimal and regional GHG emission-minimal biorefinery candidates for the three harvest and storage technologies (Fig. 12-14) were found to remain at the same location as in the baseline (Fig. 8). The locations for the alternative optimal biorefinery candidates were the same for the square bale system and square bale with no DML during storage when compared with the baseline. However, the alternative optimal biorefinery candidate for the round bale system, O_2, was in Tipton County, west Tennessee (Fig. 13), which was also close to the location of the alternative optimal biorefinery candidate O_0 in baseline (Fig. 9).

The influence of DML decomposition on the cost and GHG emissions of the switchgrass supply chain can be analyzed from three perspectives: First, when the harvest and storage technology remains the same, i.e. the baseline and Scenario 1-a, the GHG emissions of the switchgrass supply chain increase significantly due to the consideration of GHG emissions from DML decomposition. However, the slopes of the regional tradeoff curves of the baseline and Scenario 1-a (see Fig. 15) were identical, indicating that the consideration of GHG emissions from the DML decomposition would not alter the tradeoff relationship between cost and GHG emission objectives given fixed harvest and storage technology. In fact, the GHG emissions from DML decomposition were constantly a value of 195,692 CO_2e Mg.

Second, when the harvest and storage technology changed, (e.g. from the baseline to Scenario 1-b and from the baseline to Scenario 1-c), both cost and GHG emissions from the switchgrass supply chain altered. With the round bale system (Scenario 1-b), the DML rate during switchgrass storage was lower than with the square bale system, leading to less DML decomposition and associated GHG emissions. On the other hand, the round bale system was more expensive for harvest and transportation. As a result, the cost for Scenario 1-b was higher than the baseline.

With the square bale system and no DML during storage (Scenario 1-c), the GHG emissions from DML during storage could be mitigated and less switchgrass needed to be produced. As a result, cost and GHG emissions from the feedstock supply chain were reduced. Fig. 16 shows that the GHG emissions from DML decomposition were positively related to the DML rate among different harvest and storage technologies. Since GHG emissions from DML decomposition were neglected in the baseline when estimating the GHG emissions of the switchgrass supply chain, the associated value for the baseline is zero in Fig. 16. The total DML rate for Scenarios 1-a, 1-b, and 1-c were 10%, 7%, and 2%, respectively. The respective GHG emissions from these three were 195,692 CO_2e Mg, 144,538 CO_2e Mg, and 37,821 CO_2e Mg, respectively.

Third, different harvest and storage technologies also affected the density of the feedstock supply region. Fig. 17 shows the number of crop zones providing switchgrass to the biorefinery under different harvest and storage technologies for the three selected biorefinery candidates. Taking the regional cost-minimal biorefinery candidate (A_3) as examples, most crop zones were converted using the square bale system (the baseline and Scenario 1-a). The round bale system (Scenario 1-b) had less crop zones converted and the square bale system with no DML during storage (Scenario 1-c) had the least crop zones. The same pattern existed for the regional GHG emission-minimal biorefinery candidate (B_3) and regional alternative optimal biorefinery candidate (O_3).

Despite both cost and GHG emissions from the switchgrass supply chain changing according to the different harvest and storage technologies adopted, the three harvest and storage technologies examined in the sensitivity analysis were found not to change the tradeoff relationship significantly since the slope of the tradeoff curves remained the same (Fig. 15). In summary, consideration of DML decomposition led to significant net GHG emissions. However, the GHG emissions from DML were determined by the harvest and storage technology and the related DML rate during storage.

5.3 Output for Scenario 2: GHG Emissions from Cattle

The effects of considering emissions from cattle on the estimated cost and GHG emissions from the switchgrass supply chain are shown in Tables 9 and 10. Table 9 summarizes the cost and GHG emissions of the regional cost-minimal solution point (A_4^C), regional GHG emission-minimal solution point (B_4^E), and the regional alternative optimal solution point (O_4^I) when half of the cattle in the study area were migrated (i.e., PAS_{hay} equals 50%) in Scenario 2-a. Table 10 summarizes the three selected solution points, i.e., A_5^C, B_5^E, and O_5^I in Scenario 2-b in which a quarter of the cattle were migrated (i.e., PAS_{hay} equals 25%).

In Table 9, the total cost for the regional cost-minimal solution point A_4^C in Scenario 2-a was the same as that of the baseline (A_0^C) since the cost objective remained the same and the cost of cattle relocation was not considered. The associated GHG emissions for A_4^C were nearly -80,000 CO_2e Mg, which was a significant switch compared with the 82,000 CO_2e Mg GHG emissions for A_0^C in the baseline. Specifically, GHG emissions from cattle were -160,000 CO_2e Mg for A_4^C. The regional GHG emission-minimal solution point (B_4^E) and the regional alternative optimal solution point (O_4^I) had much lower cost compared with the B_0^E and O_0^I in the baseline, respectively. The opportunity cost was attributed to the reduction in cost from the baseline to Scenario 2-a. Taking the regional GHG emission-minimal solution points in the baseline and Scenario 2-a (B_0^E and B_4^E) as an example, the opportunity cost for B_4^E was only $2 million while the opportunity cost for B_0^E was above $42 million. The GHG emissions in the feedstock supply region were sequestrated by 229,000 and 204,000 for the solution points B_4^E and O_4^I, respectively.

When only a quarter of cattle were allowed to be migrated ($PAS_{hay} = 25\%$) in Scenario 2-b, the regional cost-minimal solution point (A_5^C) was $47 million, higher than the cost from baseline (A_0^C). The GHG emissions for solution point A_5^C were about -77,000 CO_2e Mg (Table 10). Costs for the regional GHG emission-minimal solution point (B_5^E) and alternative optimal solution point (O_5^I) were about $54 million and $50 million, respectively. GHG emissions for the regional GHG emission-minimal solution point (B_5^E) and alternative optimal solution point (O_5^I) were about -162,000 and -160,000 CO_2e Mg, respectively.

The locations for the regional cost-minimal biorefinery candidate, GHG emission-minimal biorefinery candidate, and the alternative optimal biorefinery candidate were showed in Figs. 18-21. For both Scenario 2-a and 2-b, the regional cost-minimal biorefinery candidates remained in Rutherford County, middle Tennessee. However, the regional GHG emission-minimal biorefinery candidates and regional alternative optimal biorefinery candidates shifted to Sullivan County, northeast Tennessee after considering the GHG emissions from cattle migration to other regions.

Fig. 22(a) shows the GHG emissions from Scenarios 2-a, 2-b and the baseline for solution points of the three selected biorefinery candidates. By assuming the cattle were moved out of the supply region, significant GHG emission reductions were observed for all the three selected biorefinery candidates. The consideration of cattle relocation also changed the priority between hay and pasture land and traditional cropland. In the baseline, hay and pasture land was chosen over cropland when considering only its cheaper economic cost. Conversely, hay and pasture land was not preferred to cropland in light of GHG emissions since the conversion of cropland to switchgrass led to high carbon sequestration. In Scenario 2-a and 2-b, since the conversion of hay and pasture land into switchgrass benefited from the emission reduction due to cattle relocation, when considering only GHG emissions, the comparative advantage of hay and pasture was even greater than cropland. As in Fig. 22(b), the type of land conversion from hay and pasture dominated in Scenarios 2-a and 2-b for all the three selected biorefinery candidates however such land use change only dominated the regional cost-minimal biorefinery candidate in baseline.

The change of priority among different crop types influenced the cost and GHG emissions of the switchgrass supply chain by changing the location of the biorefinery, the type of land conversion, and the density of supply region. Specifically, considering cattle emissions, hay and pasture land with higher density of cattle (head/acre) would be preferable for minimizing GHG emissions. Fig. 7 shows the cattle density in the study area. Hay and pasture land in northeast Tennessee were shown to have a higher cattle density compared with west Tennessee, explaining why the regional GHG emission-minimal biorefinery candidate and alternative optimal biorefinery candidates lay in Sullivan County, northeast Tennessee for Scenario 2-a and 2-b (see Fig. 19 and Fig. 21).

Also, since hay and pasture land were preferred considering cost minimization and GHG emissions, land conversion from hay and pasture land would be the dominant type for switchgrass production. Given that the variation in cost, as shown in the baseline, mainly came from the opportunity cost due to the proportion of change among different types of land conversion (see Fig. 11), such variation of cost would be insignificant in Scenario 2, in which the majority of land for switchgrass production came from hay and pasture land for the regional cost-minimal biorefinery candidates, regional GHG emission-minimal biorefinery candidates, and alternative optimal biorefinery candidates. Fig. 23 shows the regional tradeoff curves for Scenarios 2-a, 2-b, and the baseline. The regional tradeoff curves for Scenario 2-a and 2-b were flatter than that of the baseline, indicating that without much increase in economic cost, the GHG emissions of the switchgrass supply could be significantly reduced.

Furthermore, the density of the feedstock supply region was also significantly different comparing the regional GHG emission-minimal and alternative optimal biorefinery candidates between the baseline and Scenarios 2-a and 2-b. In the baseline, a total of 133 and 176 crop zones were converted into switchgrass production for the regional GHG emission-minimal biorefinery candidate and the alternative optimal biorefinery candidate, respectively. However, in Scenario 2-a, the number of crop zones increased to 809 and 508, respectively. As for Scenario 2-b, since only 25% of the cattle were allowed to be migrated out of the region, the hay and pasture land in crop zones further away were converted, reaching 1,183 for the regional GHG emission-minimal candidate and 1,168 for the regional alternative optimal biorefinery candidate (see Fig. 24).

Chapter 6 Conclusion

Biofuel generated from LCB feedstock has the potential to provide sustainable energy for future transportation with less influence on food supply and price compared with corn. However, the sustainability of LCB-based biofuel still depends on the economic and environmental performance of its feedstock supply chain. The objectives of this study were to examine the optimal design of the feedstock supply chain, specifically evaluating the tradeoffs between the objectives of cost and GHG emissions. A case study was conducted using switchgrass as the feedstock for biofuel production in Tennessee with a multi-objective mathematical model minimizing both cost and GHG emissions from the switchgrass supply chain. The augmented ε-constraint method was used to generate the tradeoff curve to reveal the tradeoffs between the two objectives under consideration.

The results showed that a tradeoff relationship existed between the cost and GHG emissions from the switchgrass supply chain. The regional cost-minimal biorefinery candidate was in Rutherford County, middle Tennessee with a total cost of $46 million and total GHG emission of 81,000 CO_2e Mg. The biorefinery candidate with regional minimal GHG emissions was in Obion County, west Tennessee with a cost of $85 million and GHG emissions of 29,000 CO_2e Mg. By allowing for a 10% increase of cost compared with the regional minimal cost candidate, the regional alternative optimal biorefinery candidate was in Haywood County, west Tennessee, with a cost of $51 million and GHG emissions of 35,000 CO_2e Mg. The imputed cost for GHG emission reduction was only $0.10/$CO_2$e kg from the regional cost-minimal biorefinery candidate to the regional alternative optimal biorefinery candidate, which was economically feasible from government subsidies. However, the imputed cost for GHG emission reduction from the regional alternative optimal biorefinery candidate to the regional GHG emission-minimal biorefinery candidate was \$6.11/CO_2e kg, which made the further GHG emissions reduction economically challenging.

Type of land that was converted to switchgrass production played an important role. On one hand, the lower opportunity cost of pasture and hay land made it preferable to traditional cropland when considering cost. On the other hand, the land conversion from traditional cropland into switchgrass was an environmentally preferred option since the land conversion from cropland to switchgrass led to net carbon sequestration while the land conversion from hayland into switchgrass released more carbon. The output was consistent with previous studies. In the study of James et al. (2010), less profitable marginal land was suggested as a means for switchgrass production to reduce opportunity cost compared with fertile land. On the other hand, the study of Kwon et al. (2013) indicated that the conversion of cropland into switchgrass led to net carbon sequestration and that the conversion of hayland released carbon in Tennessee.

Previous studies on the feedstock supply chain of biofuel also found the tradeoff relationship between the cost and GHG emissions; however, the cause of tradeoff discussed varied in the previous studies. For example, You et al. (2012) found that the structure of the supply chain network was the leading cause of the tradeoff between cost and GHG emissions of the supply chain. However, little has been done to evaluate the impact of conversion from different types of land for feedstock production on the cost and GHG emissions from the LCB feedstock supply chain.

Output from the sensitivity analysis showed the potential influence of cattle relocation and DML decomposition on the GHG emissions from the feedstock supply chain. Results suggested that DML decomposition caused considerable GHG emissions. One major factor influencing the GHG emissions from DML decomposition was the harvest and storage technologies adopted as DML rates varied during storage which then influenced GHG emissions. However, DML decomposition did not affect the relative relationship between the two objectives given the evaluated harvest and storage technologies. The assumption about the relocation of cattle due to the conversion of hay and pasture land into switchgrass had an influence not only on the GHG emissions of the switchgrass supply chain but also the tradeoff relationship between cost and GHG emissions. By assuming the cattle were relocated to places outside of the study area and addressing the consequent GHG emission change, the comparative priority between cropland and pasture and hay land was altered, making the latter more attractive from both economic and environmental perspective.

A limitation of this study is the estimation of GHG emissions from DML decomposition. The literature currently available on GHG emissions due to the decomposition of switchgrass or other LCB feedstocks is limited. The emission factor cited from Qin et al. (2006) needs further examination. Another limitation is the assumption about cattle relocation in the Scenario 2. In the baseline, it is assumed that the cattle on the converted hay and pasture land remain in the study area. That is, the density of cattle (head/acre) in the study area increases while the total cattle inventory remains the same. More fertilizer application and other operations would be needed to increase the yield of unconverted hay and pasture land; however, the associated cost was not considered in this study.

This study provides valuable information of the key factors influencing the sustainability of the LCB feedstock supply chain considering both cost and GHG emissions in Tennessee. The tradeoff relationship found between the cost and GHG emissions of the feedstock supply chain in this case study suggests that land use for feedstock production to be considered in government subsidy to motivate the development of a sustainable LCB feedstock supply chain that expedite a sustainable and commercialized advanced biofuel industry. Future studies could incorporate more criteria in the sustainable objectives, such as water usage and employment impact. Moreover, additional technologies in the LCB feedstock supply chain, such as preprocessing, could be added in the analysis. The downstream of the biofuel supply chain from biofuel production to end-use could also be incorporated when analyzing the sustainability of the biofuel industry sector.

References

AAEA. 2010. "American Agricultural Economics Association Cost and Return Handbook ".

Adler, P.R., S.J.D. Grosso, and W.J. Parton. 2007. "Life-cycle assessment of net greenhouse-gas flux for bioenergy cropping systems." *Ecological Applications* 17(3):675-691.

Archer, D.W., and J.M. Johnson. 2012. "Evaluating local crop residue biomass supply: Economic and environmental impacts." *BioEnergy Research* 5(3):699-712.

ASAE. 2006. "American Society of Agricultural Engineers Standards Agricultural Machinery Management."

Bangsund, D.A., E.A. DeVuyst, and F.L. Leistritz. 2008. "Evaluation of breakeven farm-gate switchgrass prices in south central North Dakota." North Dakota State University, Department of Agribusiness and Applied Economics. Available at: http://ageconsearch.umn.edu/bitstream/37845/2/AAE632.pdf

Bansal, A., P. Illukpitiya, S.P. Singh, and F. Tegegne. 2013. "Economic competitiveness of ethanol production from cellulosic feedstock in Tennessee." *Renewable Energy* 59:53-57.

Bernardi, A., S. Giarola, and F. Bezzo. 2012. "Spatially explicit multi-objective optimisation for the strategic design of first and second generation biorefineries including carbon and water footprints." *Industrial & Engineering Chemistry Research*. 35(9):1782-1797.

Bojarski, A.D., J.M. Laínez, A. Espuña, and L. Puigjaner. 2009. "Incorporating environmental impacts and regulations in a holistic supply chains modeling: An LCA approach." *Computers & Chemical Engineering* 33(10):1747-1759.

Bowling, I.M., J.M.a. Ponce-Ortega, and M.M. El-Halwagi. 2011. "Facility location and supply chain optimization for a biorefinery." *Industrial & Engineering Chemistry Research* 50(10):6276-6286.

Chamberlain, J.F., S.A. Miller, and J.R. Frederick. 2011. "Using DAYCENT to quantify on-farm GHG emissions and N dynamics of land use conversion to N-managed switchgrass in the Southern US." *Agriculture, Ecosystems & Environment* 141(3):332-341.

Chum, H.L., and R.P. Overend. 2001. "Biomass and renewable fuels." *Fuel processing technology* 71(1):187-195.

Cohen, M.A., and H.L. Lee. 1989. "Resource deployment analysis of global manufacturing and distribution networks." *Journal of manufacturing and operations management* 2(2):81-104.

Couclelis, H. 1991. "Requirements for planning-relevant GIS: a spatial perspective." *Regional Science* 70(1):9-19.

Crago, C.L., M. Khanna, J. Barton, E. Giuliani, and W. Amaral. 2010. "Competitiveness of Brazilian sugarcane ethanol compared to US corn ethanol." *Energy Policy* 38(11):7404-7415.

Crutzen, P.J., A.R. Mosier, K.A. Smith, and W. Winiwarter. 2008. "N_2O release from agro-biofuel production negates global warming reduction by replacing fossil fuels." *Atmospheric Chemistry and Physics* 8(2):389-395.

Cundiff, J.S., and L.S. Marsh. 1996. "Harvest and storage costs for bales of switchgrass in the southeastern United States." *Bioresource Technology* 56(1):95-101.

Cundiff, J.S., N. Dias, and H.D. Sherali. 1997. "A linear programming approach for designing a herbaceous biomass delivery system." *Bioresource Technology* 59(1):47-55.

Demirbas, A. 2007. "Progress and recent trends in biofuels." *Progress in Energy and Combustion Science* 33(1):1-18.

Dunnett, A., C. Adjiman, and N. Shah. 2007. "Biomass to heat supply chains: Applications of process optimization." *Process Safety and Environmental Protection* 85(5):419-429.

Dunnett, A.J., C.S. Adjiman, and N. Shah. 2008. "A spatially explicit whole-system model of the lignocellulosic bioethanol supply chain: an assessment of decentralised processing potential." *Biotechnology for biofuels* 1(1):1-17.

Energy Information Administration. 2013. "Cellulosic biofuel begin to flow but in lower volumes than foreseen by satatury targets." Available at: http://www.eia.gov/todayinenergy/detail.cfm?id=10131

Eksioglu, S.D., A. Acharya, L.E. Leightley, and S. Arora. 2009. "Analyzing the design and management of biomass-to-biorefinery supply chain." *Computers & Industrial Engineering* 57(4): 1342-1352.

El-Halwagi, A.M., C. Rosas, J.M. Ponce-Ortega, A. Jiménez-Gutiérrez, M.S. Mannan, and M.M. El-Halwagi. 2013. "Multiobjective optimization of biorefineries with economic and safety objectives." *AIChE Journal* 59(7): 2427-2434.

Elia, J.A., R.C. Baliban, X. Xiao, and C.A. Floudas. 2011. "Optimal energy supply network determination and life cycle analysis for hybrid coal, biomass, and natural gas to liquid (CBGTL) plants using carbon-based hydrogen production." *Computers & Chemical Engineering* 35(8):1399-1430.

Emery, I.R., and N.S. Mosier. 2012. "The impact of dry matter loss during herbaceous biomass storage on net greenhouse gas emissions from biofuels production." *Biomass and Bioenergy* 39:237-246.

English, B.C., J.A. Larson, and D.M. Mooney. 2008. “Switchgrass harvest and storage costs and bale quality”, 25th Milan No-Till Crop Production Field Day Tour Report, UT AgResearch, Knoxville, TN, pp. 11-12.

Environmental Protection Agency (EPA). 2013. "U.S. Greenhouse Gas Inventory Report." Available at: http://www.epa.gov/climatechange/ghgemissions/usinventoryreport.html

Gerloff, D. 2008. "Switchgrass Budgets." Department of Agricultural Economics, University of Tennessee. Available at: http://economics.ag.utk.edu/budgets/2009/Switchgrass2009.pdf

Giarola, S., N. Shah, and F. Bezzo. 2012. "A comprehensive approach to the design of ethanol supply chains including carbon trading effects." *Bioresource Technology* 107:175-185.

Gold, S., and S. Seuring. 2011. "Supply chain and logistics issues of bio-energy production." *Journal of Cleaner Production* 19(1):32-42.

Gorsevski, P.V., K.R. Donevska, C.D. Mitrovski, and J.P. Frizado. 2012. "Integrating multi-criteria evaluation techniques with geographic information systems for landfill site selection: a case study using ordered weighted average." *Waste management* 32(2):287-296.

Graham, R., W. Liu, H. Jager, B. English, C. Noon, and M. Daly. 1996a. “A regional-scale GIS-based modeling system for evaluating the potential costs and supplies of biomass from biomass crops”. Available at: http://www.esd.ornl.gov/~zij/mypubs/Biofuels/graham1.html

Graham, R.L., L.J. Allison, and D.A. Becker. 1996b. "ORRECL-Oak Ridge Energy Crop County Level Database." Oak Ridge National Lab., TN (US). Available at: http://www.ntis.gov/search/product.aspx?ABBR=DE2001771960

Gunderson, C.A., E.B. Davis, H.I. Jager, T.O. West, R.D. Perlack, C.C. Brandt, S. Wullschleger, L. Baskaran, E. Wilkerson, and M. Downing. 2008. "Exploring potential US switchgrass production for lignocellulosic ethanol." *ORNL/TM-2007/183, Oak Ridge National Laboratory: Oak Ridge, Tennessee*. Available at: http://gisthal.ornl.gov/sites/default/files/nagendra/KC_090916160533.pdf

Hess, J.R., T.D. Foust, R. Hoskinson, and D. Thompson. 2003. "Roadmap for agriculture biomass feedstock supply in the United States." Department of Energy (DOE). Available at: http://www.inl.gov/technicalpublications/Documents/3323197.pdf

Hess, J.R., C.T. Wright, and K.L. Kenney. 2007. "Cellulosic biomass feedstocks and logistics for ethanol production." *Biofuels, Bioproducts and biorefining* 1(3):181-190.

IPCC. 2006. "IPCC guidelines for national greenhouse gas inventories." Institute for Global Environmental Strategies, Japan. Available at: http://www.ipcc-nggip.iges.or.jp/public/2006gl/

Jackson, S. 2012. "UTBI: An Update on Progress and Future Plans." Available at: http://www.uky.edu/Ag/Forage/Jackson%2020120614_UTBI-Genera_Brief%20Overview_Keyser.pdf

James, L.K., S.M. Swinton, and K.D. Thelen. 2010. "Profitability analysis of cellulosic energy crops compared with corn." *Agronomy Journal* 102(2):675-687.

Jäppinen, E., O.-J. Korpinen, and T. Ranta. 2011. "Effects of local biomass availability and road network properties on the greenhouse gas emissions of biomass supply chain." *ISRN Renewable Energy* 2011:6.

Jäppinen, E., O.-J. Korpinen, and T. Ranta. 2013. "The Effects of Local Biomass Availability and Possibilities for Truck and Train Transportation on the Greenhouse Gas Emissions of a Small-Diameter Energy Wood Supply Chain." *BioEnergy Research* 6(1):166-177.

Kondili, E., C. Pantelides, and R. Sargent. 1993. "A general algorithm for short-term scheduling of batch operations—I. MILP formulation." *Computers & Chemical Engineering* 17(2):211-227.

Kumar, A., and S. Sokhansanj. 2007. "Switchgrass delivery to a biorefinery using integrated biomass supply analysis and logistics (IBSAL) model." *Bioresource Technology* 98(5):1033-1044.

Kwon, H.-Y., S. Mueller, J.B. Dunn, and M.M. Wander. 2013. "Modeling state-level soil carbon emission factors under various scenarios for direct land use change associated with United States biofuel feedstock production." *Biomass and Bioenergy* 55:299-310.

Larson, J.A., T.-H. Yu, B.C. English, D.F. Mooney, and C. Wang. 2010. "Cost evaluation of alternative switchgrass producing, harvesting, storing, and transporting systems and their logistics in the Southeastern USA." *Agricultural Finance Review* 70(2):184-200.

Mahmudi, H., and P.C. Flynn. 2006. "Rail vs truck transport of biomass." *Applied Biochemistry and Biotechnology* 129(1-3):88-103.

Malczewski, J. 2006. "GIS‐based multicriteria decision analysis: a survey of the literature." *International Journal of Geographical Information Science* 20(7):703-726.

Mann, M., and P. Spath. 2001. "A life cycle assessment of biomass cofiring in a coal-fired power plant." *Clean Products and Processes* 3(2):81-91.

Mas, M.D., S. Giarola, A. Zamboni, and F. Bezzo. 2010. "Capacity planning and financial optimization of the bioethanol supply chain under price uncertainty." *Computer Aided Chemical Engineering* 28:97-102.

Marvuglia, A., E. Benetto, S. Rege, and C. Jury. 2013. "Modelling approaches for consequential life-cycle assessment (C-LCA) of bioenergy: Critical review and proposed framework for biogas production." *Renewable and Sustainable Energy Reviews* 25:768-781.

Mavrotas, G. 2009. "Effective implementation of the ε-constraint method in Multi-Objective Mathematical Programming problems." *Applied Mathematics and Computation* 213(2):455-465.

Mooney, D.F., R.K. Roberts, B.C. English, D.D. Tyler, and J.A. Larson. 2009. "Yield and breakeven price of ‘Alamo’switchgrass for biofuels in Tennessee." *Agronomy Journal* 101(5):1234-1242.

Mooney, D.F., J.A. Larson, B.C. English, and D.D. Tyler. 2012. "Effect of dry matter loss on profitability of outdoor storage of switchgrass." *Biomass and Bioenergy* 44:33-41.

Morari, F., E. Lugato, and M. Borin. 2004. "An integrated non-point source model-GIS system for selecting criteria of best management practices in the Po Valley, North Italy." *Agriculture, Ecosystems & Environment* 102(3):247-262.

Nelson, R.G., C.M. Hellwinckel, C.C. Brandt, T.O. West, D.G. De La Torre Ugarte, and G. Marland. 2009. "Energy use and carbon dioxide emissions from cropland production in the United States, 1990–2004." *Journal of Environmental Quality* 38(2):418-425.

Newhart, D.D., K.L. Stott Jr, and F.J. Vasko. 1993. "Consolidating product sizes to minimize inventory levels for a multi-stage production and distribution system." *Journal of the operational Research Society* 637-644.

Ney, R., and J.L. Schnoor. 2002. "Incremental life cycle analysis: using uncertainty analysis to frame greenhouse gas balances from bioenergy systems for emission trading." *Biomass and Bioenergy* 22(4):257-269.

Noon, C.E., F.B. Zhan, and R.L. Graham. 2002. "GIS-based analysis of marginal price variation with an application in the identification of candidate ethanol conversion plant locations." *Networks and Spatial Economics* 2(1):79-93.

Parton, W. 1996. “The CENTURY model.” in *Evaluation of Soil Organic Matter Models*. Springer Berlin Heidelberg, pp. 283-291.

Perlack, R.D., and B.J. Stokes. 2011. US billion-ton update: biomass supply for a bioenergy and bioproducts industry. Oak Ridge National Laboratory. Available at: http://www1.eere.energy.gov/bioenergy/pdfs/billion_ton_update.pdf

Petrolia, D.R. 2008. "The economics of harvesting and transporting corn stover for conversion to fuel ethanol: A case study for Minnesota." *Biomass and Bioenergy* 32(7):603-612.

Qin, X., T. Mohan, M. El-Halwagi, G. Cornforth, and B.A. McCarl. 2006. "Switchgrass as an alternate feedstock for power generation: an integrated environmental, energy and economic life-cycle assessment." *Clean Technologies and Environmental Policy* 8(4):233-249.

Qin, Z., Q. Zhuang, and M. Chen. 2011. "Impacts of land use change due to biofuel crops on carbon balance, bioenergy production, and agricultural yield, in the conterminous United States." *GCB Bioenergy* 4(3): 277-288.

Rentizelas, A.A., A.J. Tolis, and I.P. Tatsiopoulos. 2009. "Logistics issues of biomass: the storage problem and the multi-biomass supply chain." *Renewable and Sustainable Energy Reviews* 13(4):887-894.

Saxton, K., W.J. Rawls, J. Romberger, and R. Papendick. 1986. "Estimating generalized soil-water characteristics from texture." *Soil Science Society of America Journal* 50(4):1031-1036.

Schimel, D., D. Ojima, M. Hartman, W. Parton, J. Brenner, A. Mosier, and S.D. Grosso. 2001. “Simulated Interaction of Carbon Dynamics and Nitrogen Trace Gas Fluxes Using the DAYCENT Model.” in S. Hansen, M. J. Shaffer, and L. Ma, ed. *Modeling Carbon and Nitrogen Dynamics for Soil Management* CRC Press.

Searchinger, T., R. Heimlich, R.A. Houghton, F. Dong, A. Elobeid, J. Fabiosa, S. Tokgoz, D. Hayes, and T.-H. Yu. 2008. "Use of US croplands for biofuels increases greenhouse gases through emissions from land-use change." *Science* 319(5867):1238-1240.

Sharma, B., R. Ingalls, C. Jones, and A. Khanchi. 2013. "Biomass supply chain design and analysis: Basis, overview, modeling, challenges, and future." *Renewable and Sustainable Energy Reviews* 24:608-627.

Smeets, E.M., I.M. Lewandowski, and A.P. Faaij. 2009. "The economical and environmental performance of miscanthus and switchgrass production and supply chains in a European setting." *Renewable and Sustainable Energy Reviews* 13(6):1230-1245.

Sokhansanj, S., A. Kumar, and A.F. Turhollow. 2006. "Development and implementation of integrated biomass supply analysis and logistics model (IBSAL)." *Biomass and Bioenergy* 30(10):838-847.

Spatari, S., Y. Zhang, and H.L. MacLean. 2005. "Life cycle assessment of switchgrass-and corn stover-derived ethanol-fueled automobiles." *Environmental science & technology* 39(24):9750-9758.

Steinitz, C., P. Parker, and L. Jordan. 1976. "Hand drawn overlays: their history and prospective uses." *Landscape Architecture* 66(5):444-455.

Thorsell, S., F.M. Epplin, R.L. Huhnke, and C.M. Taliaferro. 2004. "Economics of a coordinated biorefinery feedstock harvest system: lignocellulosic biomass harvest cost." *Biomass and Bioenergy* 27(4):327-337.

U.S. Congress. 2007. "Energy Independence and Security Act of 2007." *Office of the Press Secretary*. Available at: http://www.gpo.gov/fdsys/pkg/BILLS-110hr6enr/pdf/BILLS-110hr6enr.pdf

USDA. 2012. Soil Survey Geographical Database (SSURGO). 2012. Availble at: http://soils.usda.gov/survey/geography/ssurgo/.

USDA. National Agricultural Statistics Service. 2011. Crop Values Annual Summary. Available at: http://usda.mannlib.cornell.edu/MannUsda/viewDocumentInfo.do?documentID=1050

USDA. Farm Service Agency. 2013. “2012 acreage data as of January 2013.” Available at: http://www.fsa.usda.gov/FSA/webapp?area=newsroom&subject=landing&topic=foi-er-fri-cad.

USDA. National Agricultural Statistics Service. 2013a. Agricultural Prices. Available at: http://www.nass.usda.gov/Publications/Todays_Reports/reports/agpr0113.pdf

USDA. National Agricultural Statistics Service. 2013b. Cattle Inventory. Available at: http://www.usda.gov/nass/PUBS/TODAYRPT/catl0213.pdf

Voudouris, V.T., and A. Consulting. 1996. "Mathematical programming techniques to debottleneck the supply chain of fine chemical industries." *Computers & Chemical Engineering* 20:S1269-S1274.

Wang, M., C. Saricks, and D. Santini. 1999. "Effects of fuel ethanol use on fuel-cycle energy and greenhouse gas emissions." Available at: http://www.transportation.anl.gov/pdfs/TA/58.pdf

Wang, C., J.A. Larson, B.C. English, and K. Jensen. 2009. Cost analysis of alternative harvest, storage and transportation methods for delivering switchgrass to a biorefinery from the farmers' perspective. Master Thesis. The University of Tennessee.

Wang, M. 2010. "GREET Model: The Greenhouse Gases, Regulated Emissions, and Energy Use in Transportation Model." *Argonne National Lab.* Available at: http://greet.es.anl.gov/

Ward, D.P., A.T. Murray, and S.R. Phinn. 2003. "Integrating spatial optimization and cellular automata for evaluating urban change." *The Annals of Regional Science* 37(1):131-148.

Wilson, B.S. 2009. "Modeling Cellulosic Ethanol Plant Location Using GIS." Mater Thesis. The University of Tennessee.

Wilson, T.O., F.M. McNeal, S. Spatari, D. G. Abler, and P.R. Adler. 2011. "Densified biomass can cost-effectively mitigate greenhouse gas emissions and address energy security in thermal applications." *Environmental science & technology* 46(2):1270-1277.

Wu, J., M. Sperow, and J. Wang. 2010. "Economic feasibility of a woody biomass-based ethanol plant in Central Appalachia." *Journal of Agricultural and Resource Economics* 35(3):522.

You, F., L. Tao, D.J. Graziano, and S.W. Snyder. 2012. "Optimal design of sustainable cellulosic biofuel supply chains: Multiobjective optimization coupled with life cycle assessment and input–output analysis." *AIChE Journal* 58(4):1157-1180.

You, F., and B. Wang. 2011. "Life cycle optimization of biomass-to-liquids supply chains with distributed-centralized processing networks." *Industrial & Engineering Chemistry Research*. 50(17): 10102-10127.

Yu, T.E., B.C. English, J.A. Larson, J.S. Fu, D. De La Torre Ugarte, J. Yun, J. Calcagno III, and B. Wilson. 2013. "Modeling the Air Quality Impacts of Feedstocks Transportation for Cellulosic Biofuel Production in Tennessee." Transportation Research Board Annual Meeting, pp. 13-1650. Available at: http://amonline.trb.org/2vcs4p/1

Zhang, F., D.M. Johnson, and J.W. Sutherland. 2011. "A GIS-based method for identifying the optimal location for a facility to convert forest biomass to biofuel." Biomass and Bioenergy 35(9):3951-3961.

Zhang, J., A. Osmani, I. Awudu, and V. Gonela. 2012. "An integrated optimization model for switchgrass-based bioethanol supply chain." *Applied Energy* 102: 1205-1217.

Appendix

Table 1. Biorefinery and Feedstock Supply Chain Operation Options and Assumptions for Different Scenarios

	Baseline	Scenario 1 with DML* Emissions	Scenario 2 with Cattle Emissions
Harvest and Storage Technology	Square bale with tarp and pallet	1-a. Square bale with tarp and pallet	Square bale with tarp and pallet
		1-b. Round bale without tarp or pallet	
		1-c. Square bale with no DML during storage	
PAS_{hay} *	50%	50%	2-a. 50%
			2-b. 25%
Biorefinery conversion	76 gallons/Mg switchgrass		
Biorefinery capacity	50 million gallons per year		
Biorefinery location	Industrial parks with access to water, power, and roads, as well as sufficient storage space		
System Boundary	Field to biorefinery gate		
Harvest	November to February; No DML during switchgrass harvest		
Transportation	Semi-truck with max travelling distance of 75 miles; 2% DML during switchgrass transportation		

Note: PAS_{hay} stands for the percentage of hay and pasture land that is available for switchgrass production, DML stands for dry matter loss.

Table 2. Components for Cost and GHG Emissions from Switchgrass Supply Chain

	Economic Cost	GHG Emissions
Land Conversion	Opportunity cost	Land use change Cattle relocation*
Production	Establishment Annual maintenance	Fuel usage Fertilizer, herbicide, seed production Machine production
Harvest	Labor Fuel Machinery	Fuel usage Machine production
Storage	Labor Fuel Machinery Covers and pallets	Fuel usage Machinery production Dry matter loss decomposition*
Transportation	Labor Fuel Truck	Truck emission Truck production

Note: * indicates that the source was considered in sensitivity analysis but excluded in the baseline

Table 3. Definitions of Subscripts, Parameters and Variables

	Unit	Definition
Subscripts		
i		locations of switchgrass production field
j		location of the biorefinery
m		month
p		crops (hay & pasture, corn, soybean, wheat)
b		harvest method (square baler, round baler)
t		storage protection method
k		type of machinery (tractor, mower, loader, rake)
Parameters		
$\mathrm{Price}_{\mathrm{ip}}$	$/unit	traditional crop price
$\mathrm{Yield}_{\mathrm{ip}}$	acre/unit	tradition crop yield
$\mathrm{PC}_{\mathrm{ip}}$	$/acre	production cost of traditional crop
$Yield_i{}^{swi}$	ton/acre	yield for switchgrass in each hexagon
LR_{ip}	$/acre	land rent of traditional crop
Est	$/acre	Establishment cost in the first year
AM	$/acre	Annual maintenance cost
Sigma_{ib}	$/acre	cost of harvesting switchgrass
BEP_{ipb}	$/acre	breakeven price of land conversion to switchgrass
γ_{ibt}	$/ton	cost of storing switchgrass
θ_{ib}	$/ton	cost of transporting switchgrass from field to biorefinery
$\mathrm{lucE^{co2}{}_p}$	CO_2e kg/acre	CO_2 emission from land conversion of crop to switchgrass
$\mathrm{lucE^{n2o}{}_p}$	CO_2e kg/acre	N_2O emission from land conversion of crop to switchgrass
storE	CO_2e kg/ton	GHG emissions from energy usage during storage
$\mathrm{harE_b}$	CO_2e kg/acre	GHG emissions from energy usage during harvest
$\mathrm{proE_b}$	CO_2e kg/acre	GHG emissions from energy usage during production
$\mathrm{transE_{mip}}$	CO_2e kg /truck/route	GHG emissions from energy usage during transportation
fertE	CO_2e kg/ton	GHG emissions from fertilizer production
herbE	CO_2e kg/ton	GHG emissions from herbicide production
seedE	CO_2e kg/ton	GHG emissions from seed production
machE^k	CO_2e kg/unit	GHG emissions from machinery production
$loadwt_{mib}$	ton/truck	Tonnage of switchgrass delivered per truck
aa_{ip}	acre	cropland available in each hexagon for each crop
$CapUnit$	gal/year	annual capacity of a biorefinery
λ	gal/ton	switchgrass-ethanol conversional rate
$rateava_m$	%	ratio of working hours in each month to total
$avehour_m$	hour	average working hours of machinery in each month
mtb_{ib}	hour/acre	machine time per acre for each machinery
PAS_p	%	maximum percent of land converted
$DMLT$	%	dry matter loss during transportation

Table 3. Continued

	Unit	Definition
Parameters		
$DMLS_{mbt}$	%	dry matter loss during storage
Dd_m	gal/month	monthly demand for ethanol
τ_i	head/acre	the density of cattle one per acre of hay and pasture land
$cattleE$	CO_2e kg /head	GHG emissions from per head of cattle removed
$lossE$	CO_2e kg/ton	GHG emissions from per tonnage of lost switchgrass decompos
Variables		
A_{ipb}	acre	acres of switchgrass produced annually
AH_{mipb}	acre	acres of switchgrass harvested monthly
XC_{ipb}	ton	tons of switchgrass produced annually
XH_{mipb}	ton	tons of switchgrass harvested monthly from November to February
XTN_{mipb}	ton	tons of switchgrass transported directly to the biorefinery after harvest
NXS_{mipbt}	ton	tons of switchgrass newly stored monthly from November to February
XS_{mipbt}	ton	tons of switchgrass stored monthly from November to October
XTO_{mipbt}	ton	tons of switchgrass transported from storage to the biorefinery
${Numb_{mb}}^k$	unit	number of equipment used in harvest

Table 4. Emission Factors for Switchgrass Supply Chain (Unit: CO2e kg/acre/year if no special note)

	Items		Value	Source
Land use change CO_2 --$lucE^{co2}{}_p$	Corn		-385.84	DAYCENT
	Cotton		-377.89	
	Hay and pasture		210.46	
	Sorghum		-271.39	
	Soybean		-98.22	
	Wheat		-404.78	
Land use change N_2O --$lucE^{n2o}{}_p$	Corn		69.19	DAYCENT
	Cotton		71.06	
	Hay and pasture		117.86	
	Sorghum		78.81	
	Soybean		95.53	
	Wheat		65.96	
Farm and harvest machine [a] --$mach\mathrm{E}^k$	Tractor		985.77	GREET
	Loader		468.22	
	Baler	Square	3155.54	
		Round	1693.28	
	Mower		2111.25	
	PTO rake		615.54	
Energy consume -- $proE, harE_b, storE$	Production		33.19	GREET
	Harvest	Square	405.17	
		Round	519.18	
	Storage		2.32[b]	
Production of fertilizer, seed and herbicide --$fertE, herbE, seedE$	Fertilizer		106.49	GREET
	Seed		18.16	
	Herbicide		1.34	

Notes:
a. Unit: CO_2e kg per machinery per year
b. Unit: CO_2e kg per Mg switchgrass per year

Table 5. Cost and GHG Emissions Summary for the Solution Points at the Selected Biorefinery Candidates in Baseline

	A_0^C	B_0^E	O_0^I
Total Cost ($)	**45,968,780**	**85,330,422**	**50,565,658**
Opportunity	1,610,770	42,410,177	7,253,640
Production	8,610,561	8,718,782	8,933,278
Harvest	22,401,401	22,542,314	22,821,609
Storage	2,774,791	3,083,039	2,774,791
Transportation	10,571,257	8,576,110	8,782,338
Total GHG Emission (CO_2e Mg)	**81,564**	**29,321**	**35,007**
Soil CO_2	15,759	-31,182	-27,510
Corn	-	*(31,075)*	-
Cotton	*(663)*	*(105)*	*(28,020)*
Hay	*16,424*	-	*1,293*
Sorghum	-	-	*(777)*
Soybeans	*(2)*	-	*(6)*
Wheat	*(0)*	*(2)*	*(0)*
Soil N_2O	9,324	5,592	6,184
Corn	-	*5,572*	-
Cotton	*125*	*20*	*5,269*
Hay	*9,197*	-	*724*
Sorghum	-	-	*185*
Soybeans	*2*	-	*6*
Wheat	*0*	*0*	*0*
Energy	36,675	37,115	37,986
Est, AM	*2,649*	*2,682*	*2,748*
Harvest	*32,339*	*32,746*	*33,551*
Storage	*1,687*	*1,687*	*1,687*
Transportation	3,930	1,757	1,989
Indirect	15,876	16,037	16,356
Machinery	*5,820*	*5,855*	*5,923*
Fertilizer	*8,500*	*8,606*	*8,818*
Herbicide	*107*	*108*	*111*
Seed	*1,449*	*1,468*	*1,504*
Total Harvested Feedstock (Ton)	**727,366**	**727,366**	**727,366**
Total Land Converted (Acre)	**79,816**	**80,819**	**82,808**
Hay & Pasture Land Ratio (%)	**97.8**	**0**	**7.4**
No. of Crop Zone	**406**	**133**	**176**

Table 6. Cost and GHG Emissions Summary for Solution Points at the Selected Biorefinery Candidates in Scenario 1-a with Square Bale System

	A_1^C	**B_1^E**	**O_1^I**
Total Cost ($)	**45,968,780**	**85,330,422**	**50,565,658**
Opportunity	1,610,770	42,410,177	7,253,640
Production	8,610,561	8,718,782	8,933,278
Harvest	22,401,401	22,542,314	22,821,609
Storage	2,774,791	3,083,039	2,774,791
Transportation	10,571,257	8,576,110	8,782,338
Total GHG Emission (CO_2e Mg)	**277,256**	**225,013**	**230,698**
Soil CO_2	15,759	-31,182	-27,510
Corn	-	*(31,075)*	-
Cotton	*(663)*	*(105)*	*(28,020)*
Hay	*16,424*	-	*1,293*
Sorghum	-	-	*(777)*
Soybeans	*(2)*	-	*(6)*
Wheat	*(0)*	*(2)*	*(0)*
Soil N_2O	9,324	5,592	6,184
Corn	-	*5,572*	-
Cotton	*125*	*20*	*5,269*
Hay	*9,197*	-	*724*
Sorghum	-	-	*185*
Soybeans	*2*	-	*6*
Wheat	*0*	*0*	*0*
Energy	36,675	37,115	37,986
Est, AM	*2,649*	*2,682*	*2,748*
Harvest	*32,339*	*32,746*	*33,551*
Storage	*1,687*	*1,687*	*1,687*
Transportation	3,930	1,757	1,989
Indirect	15,876	16,037	16,356
Machinery	*5,820*	*5,855*	*5,923*
Fertilizer	*8,500*	*8,606*	*8,818*
Herbicide	*107*	*108*	*111*
Seed	*1,449*	*1,468*	*1,504*
DML	195,692	195,692	195,692
Total Harvested Feedstock (Ton)	**727,366**	**727,366**	**727,366**
Total Land Converted (Acre)	**79,816**	**80,819**	**82,808**
Hay & Pasture Land Ratio (%)	**97.8**	**0**	**7.4**
No. of Crop Zone	**406**	**133**	**176**

Table 7. Cost and GHG Emissions Summary for Solutions Points at the Selected Biorefinery Candidates in Scenario 1-b with Round Bale System

	A_2^C	B_2^E	O_2^I
Total Cost ($)	**48,246,067**	**85,843,722**	**53,070,674**
Opportunity	1,628,030	41,342,249	7,804,646
Production	8,395,753	8,500,764	8,767,142
Harvest	24,708,521	24,836,534	25,161,254
Storage	-	-	-
Transportation	13,513,764	11,164,174	11,337,632
Total GHG Emission (CO_2e Mg)	**234,334**	**183,618**	**188,471**
Soil CO_2	14,846	(30,400)	(28,082)
Corn	*(1)*	*(30,275)*	-
Cotton	*(978)*	*(124)*	*(28,945)*
Hay	*15,827*	-	*932*
Sorghum	-	-	*(66)*
Soybeans	*(3)*	-	*(3)*
Wheat	*(0)*	*(1)*	*(0)*
Soil N_2O	9,050	5,452	5,984
Corn	*0*	*5,429*	
Cotton	*184*	*23*	*5,443*
Sorghum	-	-	*16*
Hay	*8,863*	-	*522*
Soybeans	*3*	-	*3*
Wheat	*0*	*0*	*0*
Energy	44,634	45,171	46,535
Est, AM	*2,649*	*2,682*	*2,748*
Harvest	*32,339*	*32,746*	*33,551*
Storage	*1,687*	*1,687*	*1,687*
Transportation	4,685	2,120	2,367
Indirect	16,582	16,737	17,129
Machinery	*6,777*	*6,809*	*6,890*
Fertilizer	*8,287*	*8,391*	*8,654*
Herbicide	*104*	*106*	*109*
Seed	*1,413*	*1,431*	*1,476*
DML	144,538	144,538	144,538
Total Harvested Feedstock (Ton)	**709,206**	**709,206**	**709,206**
Total Land Converted (Acre)	**77,825**	**78,798**	**81,268**
Hay & Pasture Land Ratio (%)	**96.6**	**0**	**5.5**
No. of Crop Zone	**396**	**122**	**116**

Table 8. Cost and GHG Emissions Summary for Solution Points at the Selected Biorefinery Candidates in Scenario 1-c with Square Bale System and no DML during Storage

	A_3[C]	**B_3[E]**	**O_3[I]**
Total Cost ($)	**43,093,145**	**79,552,385**	**47,402,460**
Opportunity	1,496,150	39,087,036	6,891,721
Production	7,946,690	8,048,238	8,243,698
Harvest	20,674,804	20,807,028	21,061,534
Storage	2,465,986	3,098,605	2,465,986
Transportation	10,509,514	8,511,478	8,739,521
Total GHG Emission (CO_2e Mg)	**113,247**	**64,993**	**68,666**
Soil CO_2	14,466	(28,782)	(26,821)
Corn	-	*(28,676)*	-
Cotton	*(662)*	*(105)*	*(26,730)*
Hay	*15,130*	-	*680*
Sorghum	-	-	*(769)*
Soybeans	*(2)*	-	*(2)*
Wheat	*(0)*	*(1)*	*(0)*
Soil N_2O	8,599	5,162	5,592
Corn	-	*5,142*	-
Cotton	*124*	*20*	*5,026*
Hay	*8,473*	-	*381*
Sorghum	-	-	*183*
Soybeans	*2*	-	*2*
Wheat	*0*	*0*	*0*
Energy	33,848	34,261	35,055
Est, AM	*2,445*	*2,476*	*2,536*
Harvest	*29,846*	*30,227*	*30,961*
Storage	*1,557*	*1,557*	*1,557*
Transportation	3,838	1,705	1,901
Indirect	14,676	14,827	15,118
Machinery	*5,395*	*5,428*	*5,490*
Fertilizer	*7,844*	*7,945*	*8,137*
Herbicide	*99*	*100*	*102*
Seed	*1,338*	*1,355*	*1,388*
DML	37,821	37,821	37,821
Total Harvested Feedstock (Ton)	**671,321**	**671,321**	**671,321**
Total Land Converted (Acre)	**73,662**	**74,604**	**76,415**
Hay & Pasture Land Ratio (%)	**97.6**	**0.0**	**4.2**
No. of Crop Zone	**378**	**118**	**125**

Table 9. Cost and GHG Emissions Summary for Solution Points at the Selected Biorefinery Candidates in Scenario 2-a with PAS_{hay} Equals 50%

	A_4^C	B_4^E	O_4^I
Total Cost ($)	**45,968,780**	**54,321,204**	**50,565,658**
Opportunity	1,610,770	2,028,857	2,082,871
Production	8,610,561	9,637,241	9,417,575
Harvest	22,401,401	23,738,232	23,452,207
Storage	2,774,791	2,909,756	2,774,791
Transportation	10,571,257	16,007,119	12,838,214
Total GHG Emission (CO_2e Mg)	**(79,176)**	**(229,011)**	**(204,339)**
Soil CO_2	15,759	24,045	23,434
Corn	-	-	-
Cotton	*(663)*	-	-
Hay	*16,424*	*24,045*	*23,434*
Sorghum	-	-	-
Soybeans	*(2)*	-	-
Wheat	*(0)*	-	-
Soil N_2O	9,324	13,466	13,123
Corn	-	-	-
Cotton	*125*	-	-
Hay	*9,197*	*13,466*	*13,123*
Sorghum	-	-	-
Soybeans	*2*	-	-
Wheat	*0*	-	-
Energy	36,675	51,770	50,497
Est, AM	*2,649*	*3,792*	*3,696*
Harvest	*32,339*	*46,291*	*45,114*
Storage	*1,687*	*1,687*	*1,687*
Transportation	3,930	9,668	6,978
Indirect	15,876	22,313	21,815
Machinery	*5,820*	*7,918*	*7,787*
Fertilizer	*8,500*	*12,167*	*11,857*
Herbicide	*107*	*153*	*149*
Seed	*1,449*	*2,075*	*2,022*
Cattle	(160,740)	(350,273)	(320,188)
Total Harvested Feedstock (Ton)	**727,366**	**727,366**	**727,366**
Total Land Converted (Acre)	**79,816**	**114,252**	**111,347**
Hay & Pasture Land Ratio (%)	**97.8**	**100**	**100**
No. of Crop Zone	**406**	**809**	**508**

Table 9. Cost and GHG Emissions Summary for Solution Points at the Selected Biorefinery Candidates in Scenario 2-a with PAS_{hay} Equals 25%

	A_4^C	B_4^E	O_4^I
Total Cost ($)	**47,641,023**	**53,052,286**	**52,405,125**
Opportunity	1,729,581	1,844,227	1,836,993
Production	8,609,191	9,294,554	9,289,013
Harvest	22,399,618	23,292,022	23,284,807
Storage	2,774,791	2,931,338	2,781,744
Transportation	12,127,841	15,690,145	15,212,568
Total GHG Emission (CO_2e Mg)	**(77,507)**	**(161,663)**	**(160,365)**
Soil CO_2	15,017	20,755	20,652
Corn	*(8)*	-	-
Cotton	*(1,125)*	-	-
Hay	*16,150*	*20,755*	*20,652*
Sorghum	-	-	-
Soybeans	*(6)*	-	-
Wheat	*(2)*	-	-
Soil N_2O	9,264	11,623	11,566
Corn	*1*	-	-
Cotton	*212*	-	-
Hay	*9,045*	*11,623*	*11,566*
Sorghum	-	-	-
Soybeans	*6*	-	-
Wheat	*0*	-	-
Energy	36,670	44,917	44,704
Est, AM	*2,649*	*3,273*	*3,257*
Harvest	*32,334*	*39,956*	*39,759*
Storage	*1,687*	*1,687*	*1,687*
Transportation	5,400	9,530	9,436
Indirect	15,874	19,347	19,255
Machinery	*5,819*	*6,922*	*6,891*
Fertilizer	*8,498*	*10,502*	*10,450*
Herbicide	*107*	*132*	*131*
Seed	*1,449*	*1,791*	*1,782*
Cattle	(159,724)	(267,835)	(265,977)
Total Harvested Feedstock (Ton)	**727,366**	**727,366**	**727,366**
Total Land Converted (Acre)	**79,803**	**98,616**	**98,130**
Hay & Pasture Land Ratio (%)	**96.2**	**100**	**100**
No. of Crop Zone	**831**	**1183**	**1168**

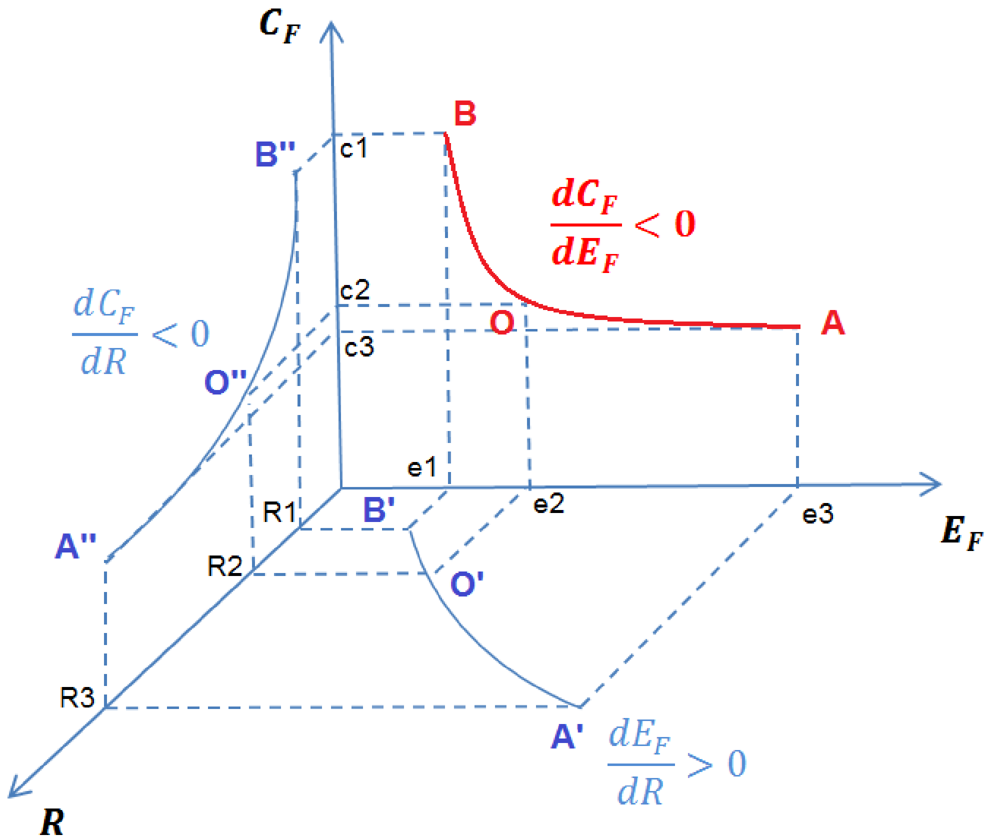

Figure 1. Tradeoff between cost and GHG emissions due to type of land conversion

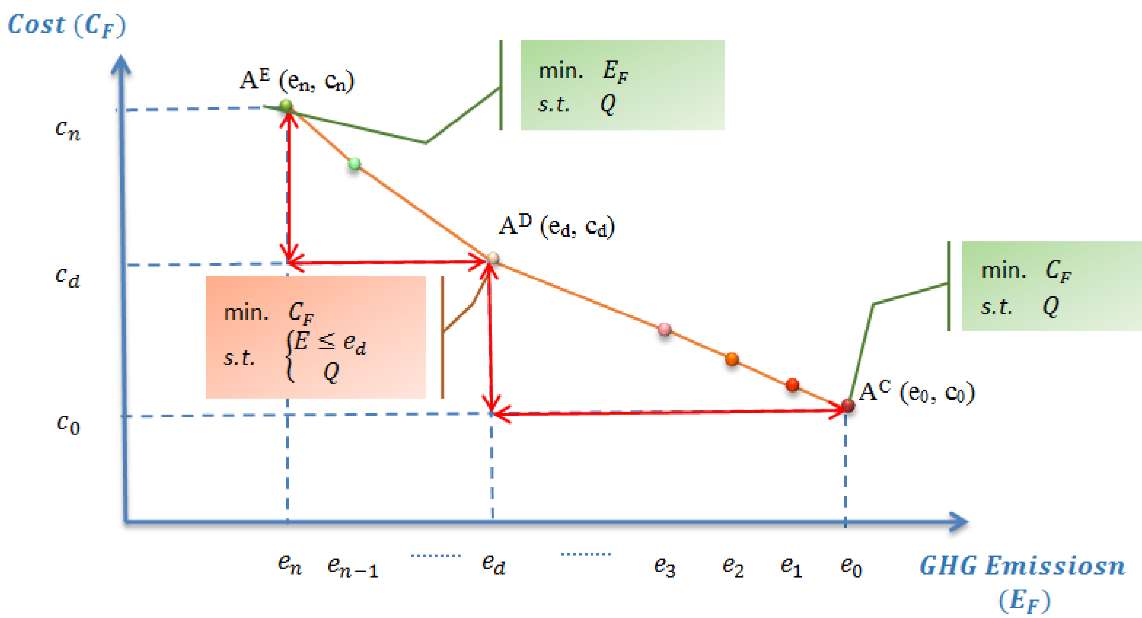

Figure 2. Single-location tradeoff curve

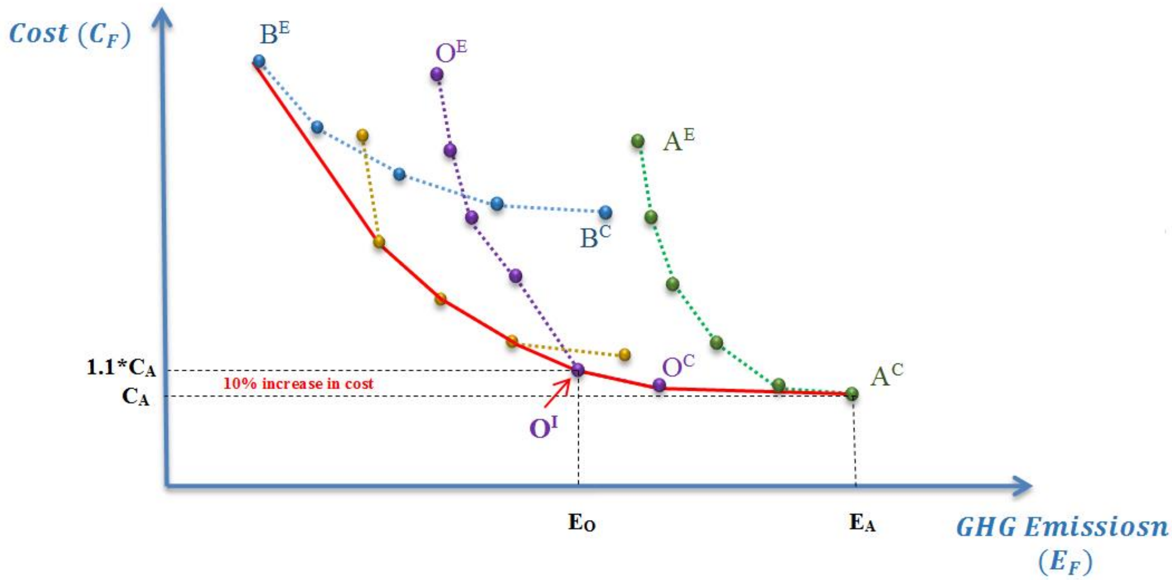

Figure 3. Regional tradeoff curve

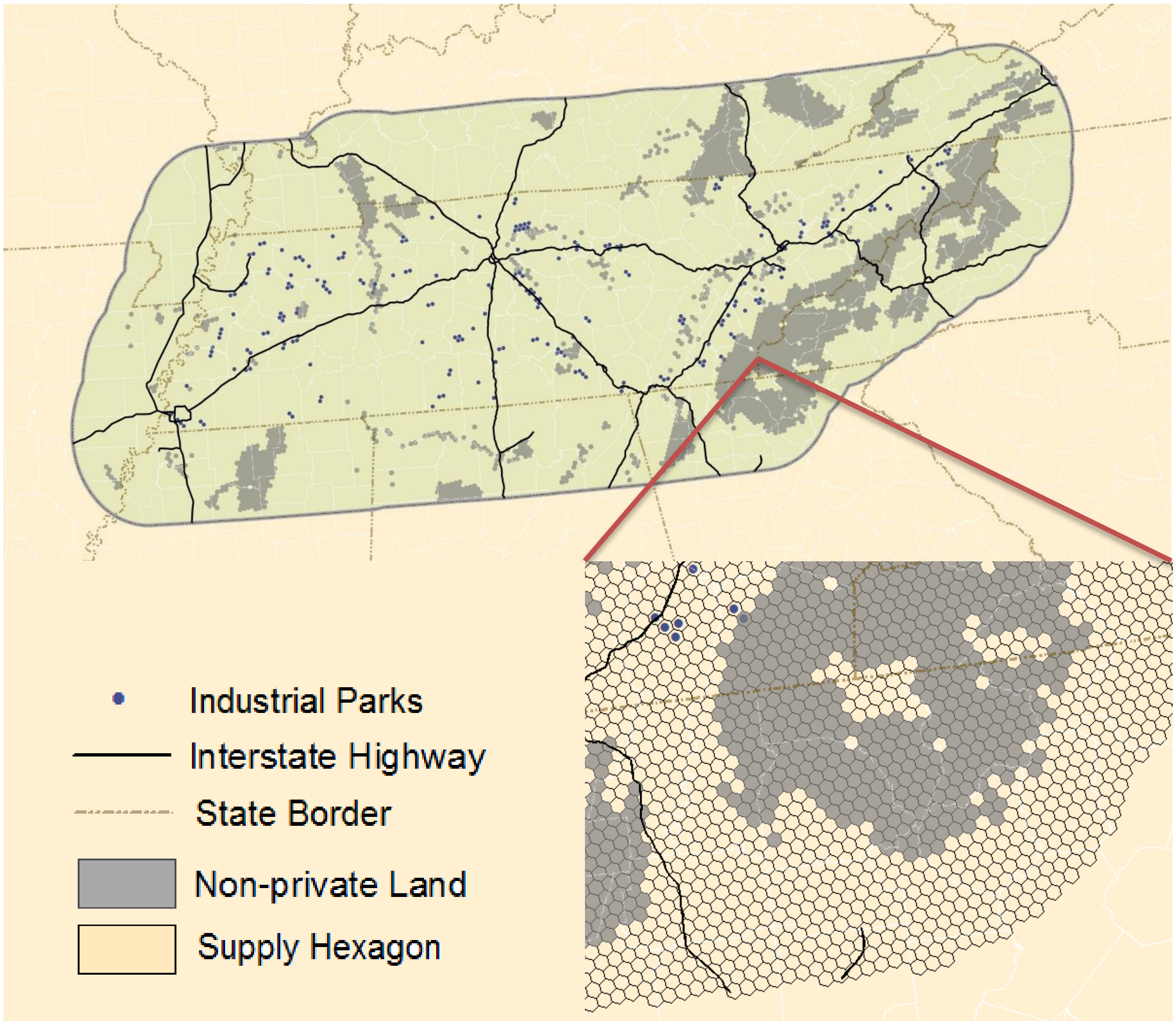

Figure 4. Study area of Tennessee in crop zone level

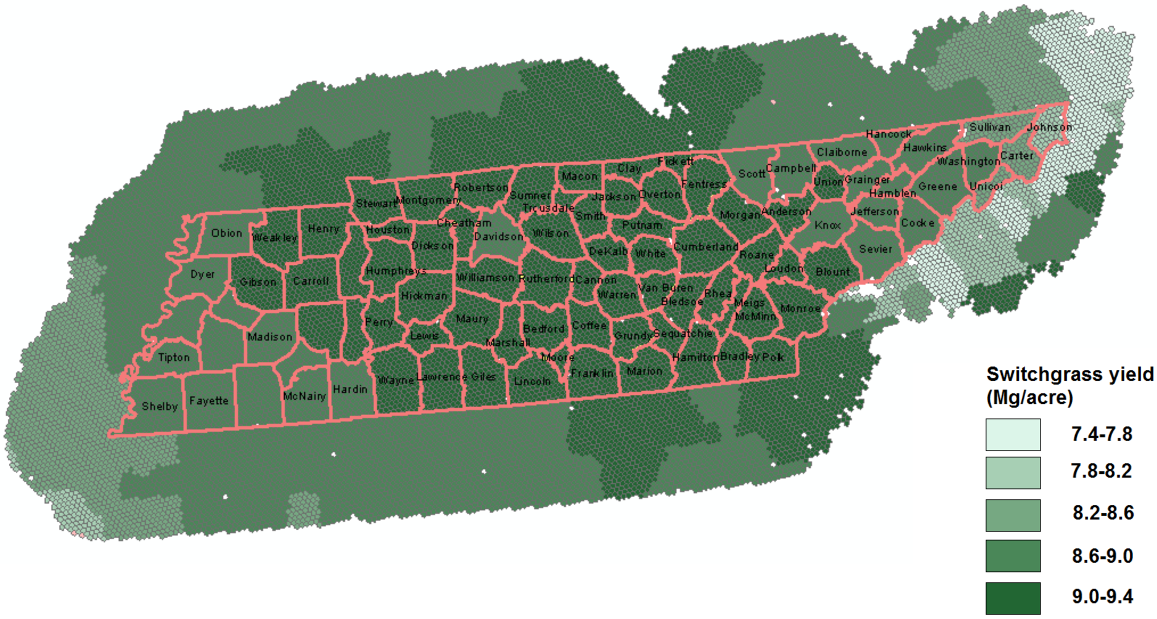

Figure 5. Switchgrass yield of the study area in crop zone level

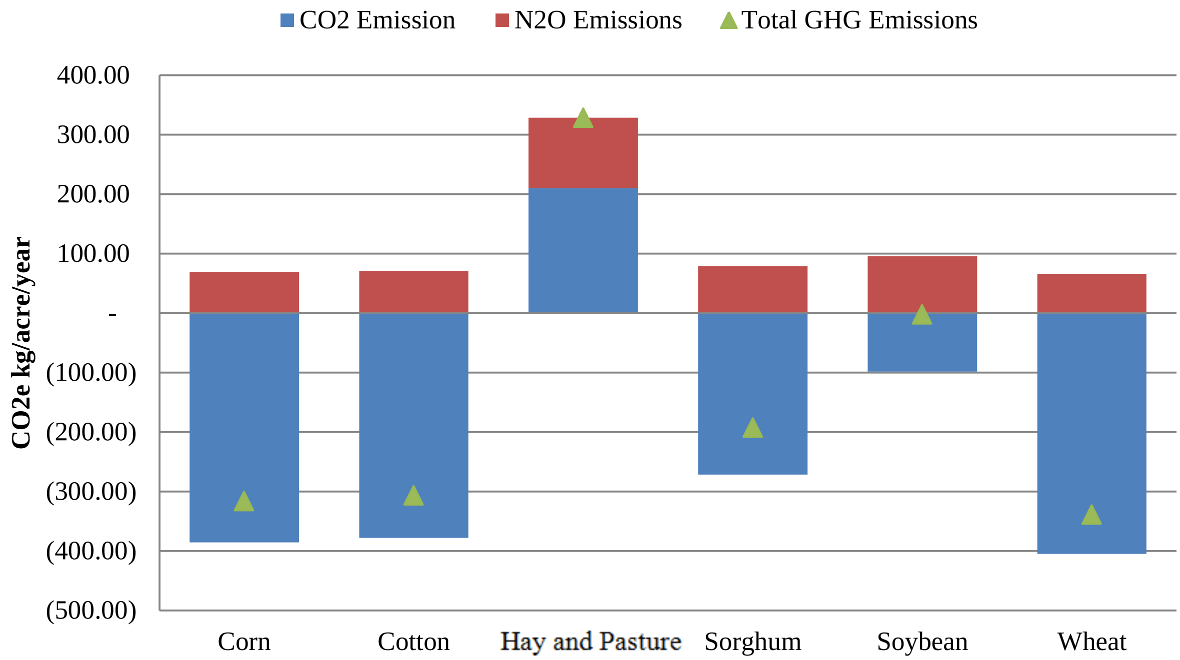

Figure 6. GHG emissions change converting different crops into switchgrass from DAYCENT

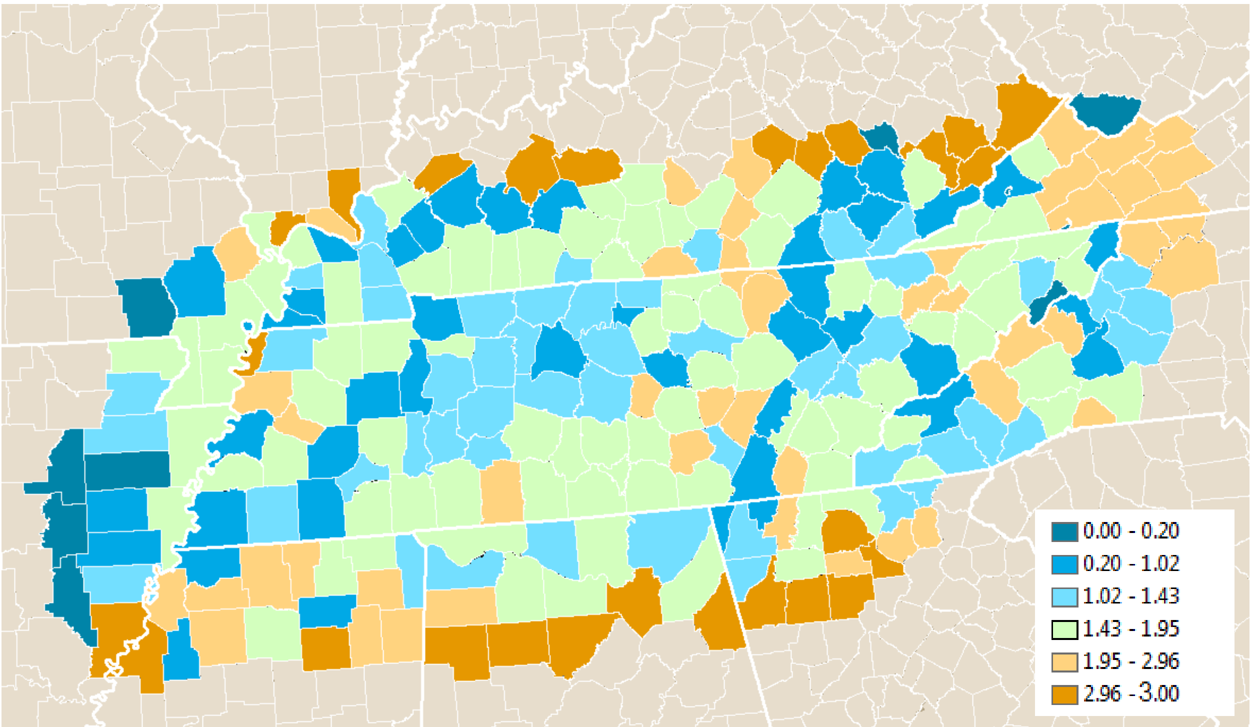

Figure 7. The density of cattle on hay and pasture land (head/acre) for the counties in the study area

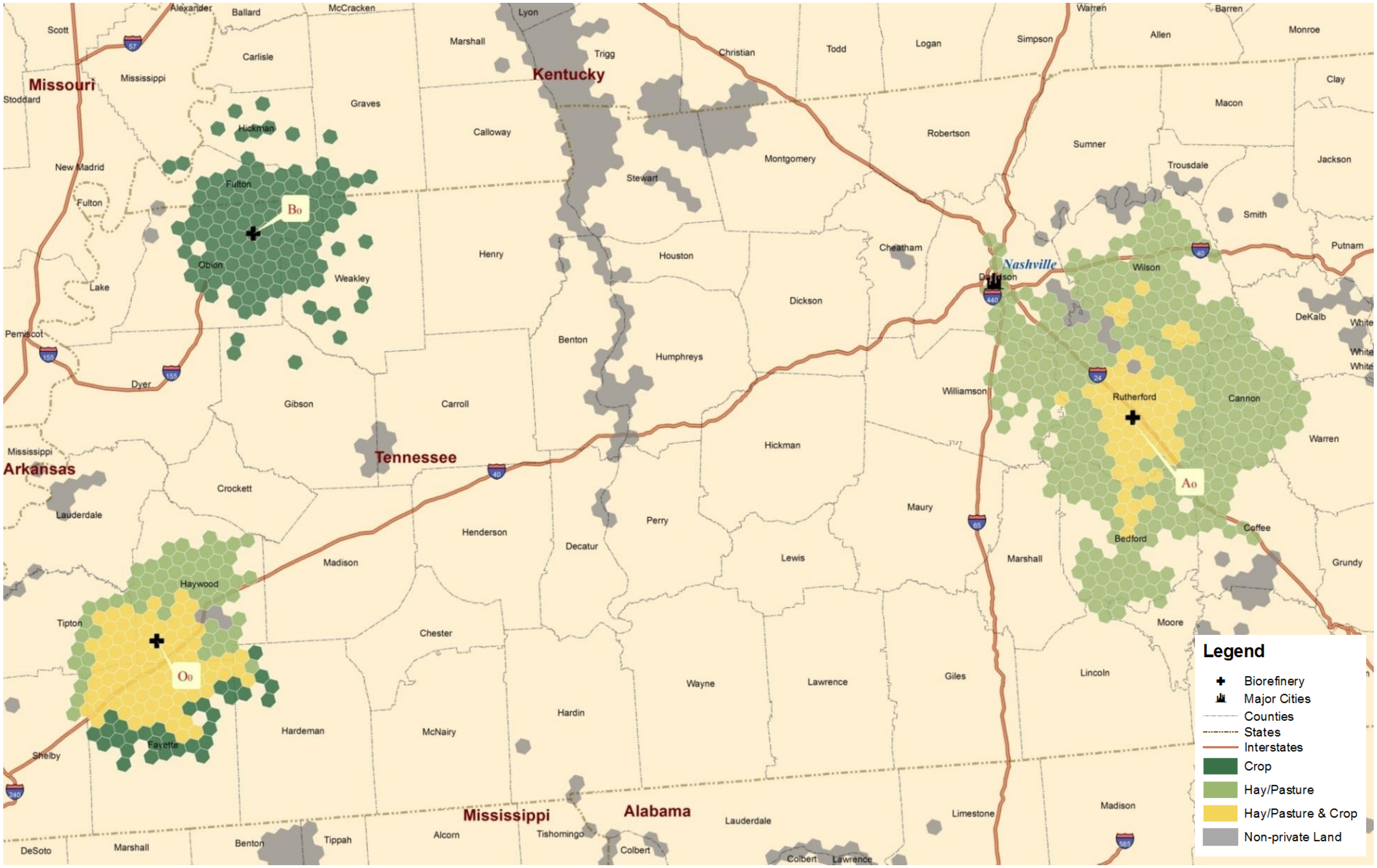

Figure 8. Location of biorefinery and associated supply region for the three selected biorefinery candidates in baseline

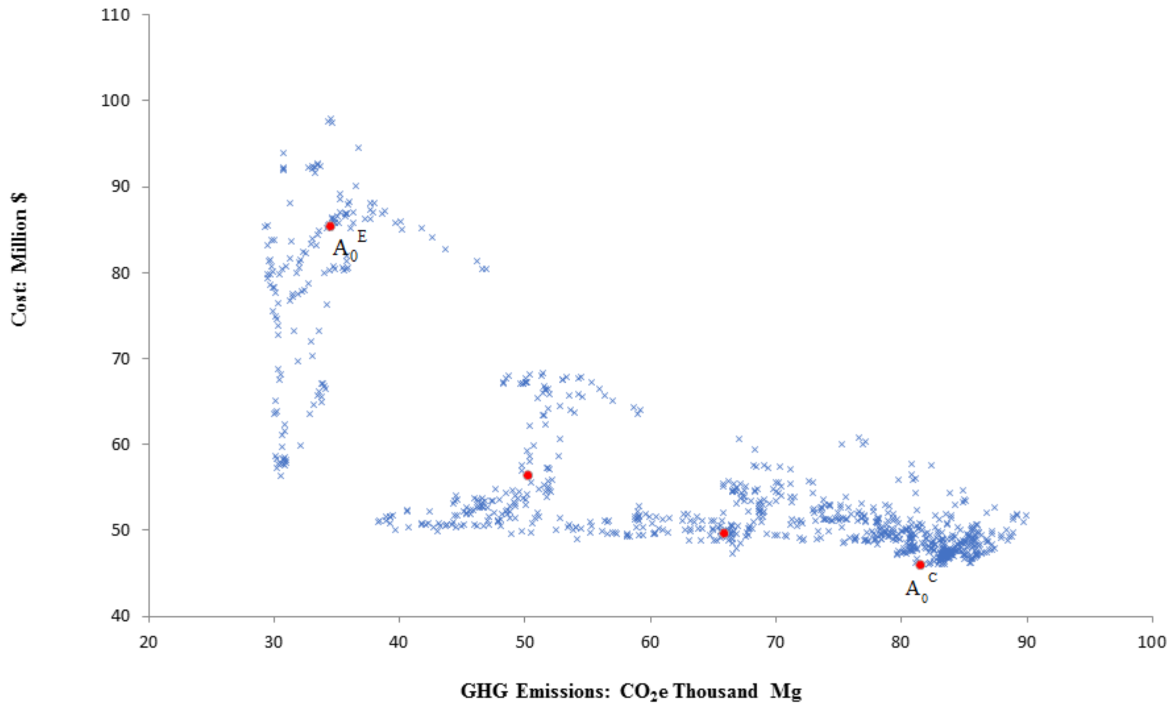

Figure 9. The solution points for the baseline

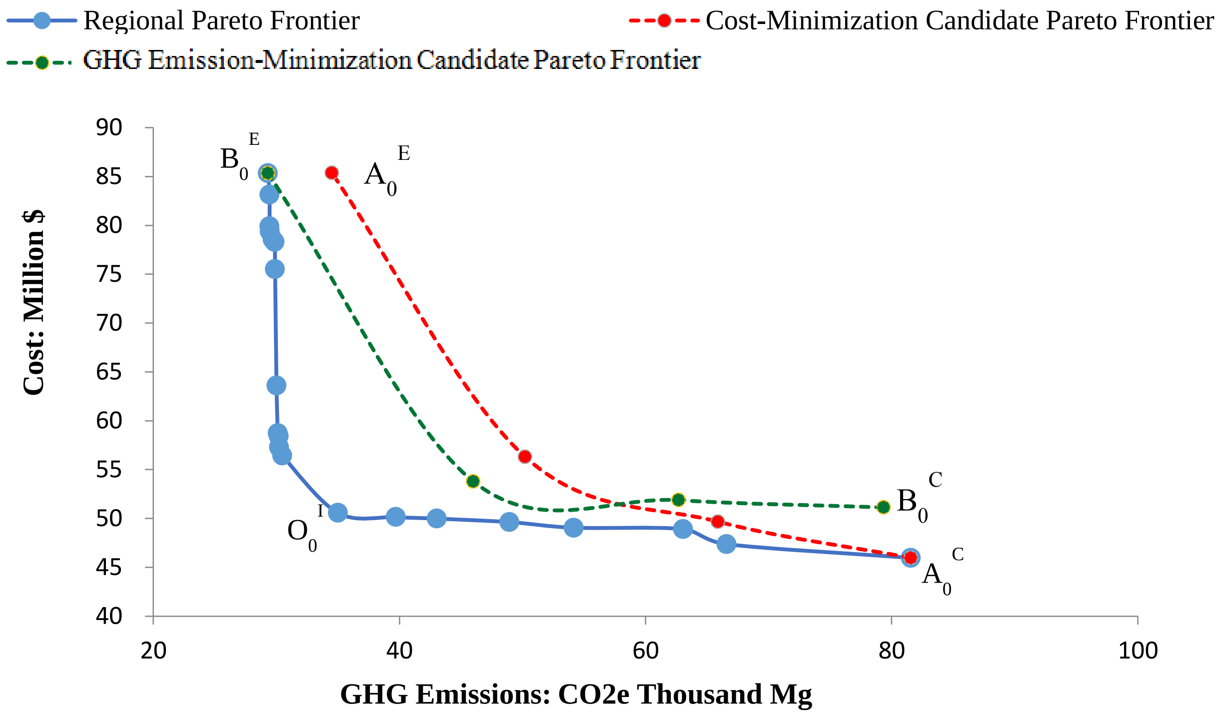

Figure 10. The tradeoff curves for three selected biorefinery candidates in baseline and the regional tradeoff curve

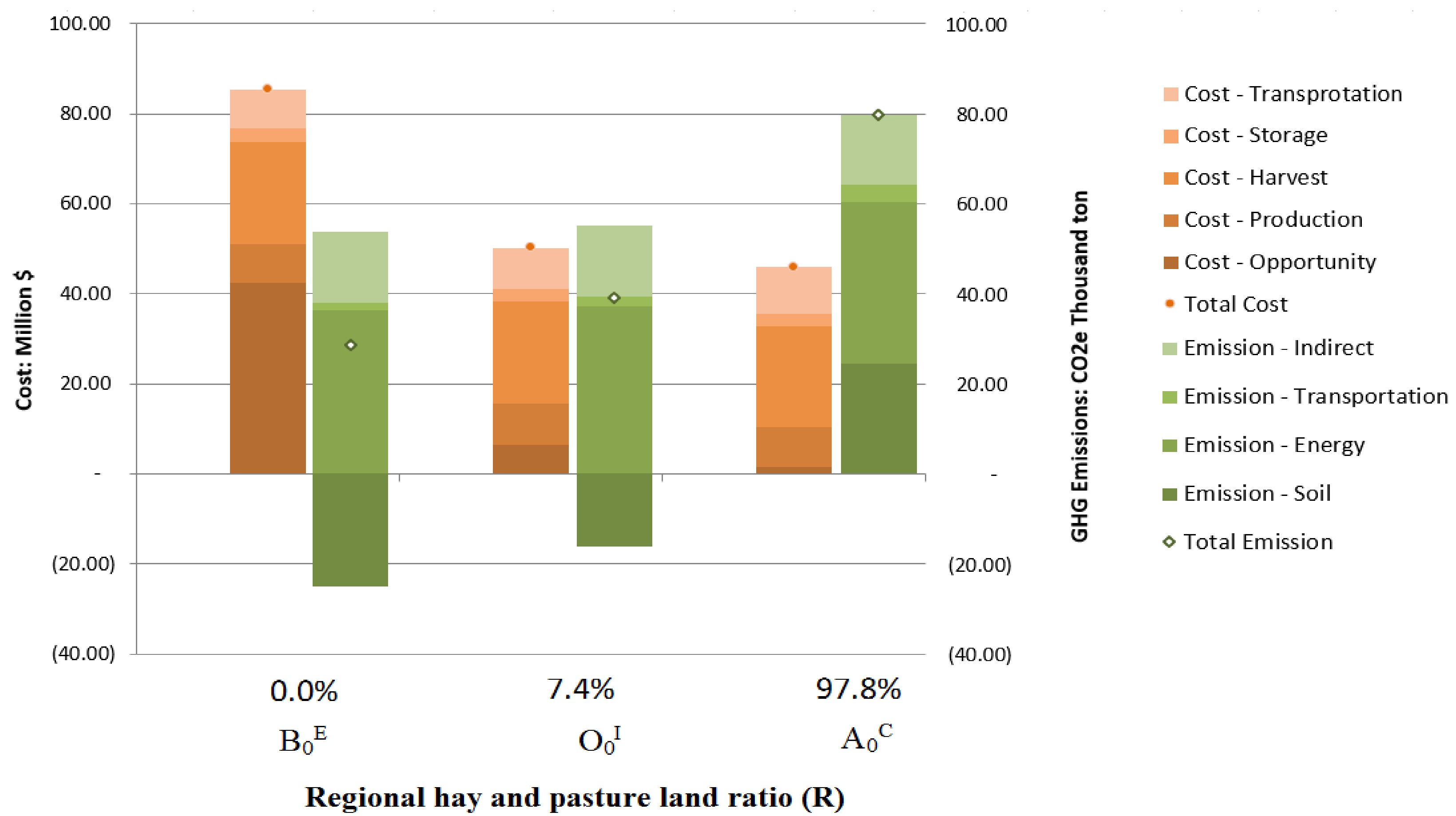

Figure 11. Comparison of cost, GHG emissions and percentage of hay and pasture land converted in total land converted of the three biorefinery candidates in baseline

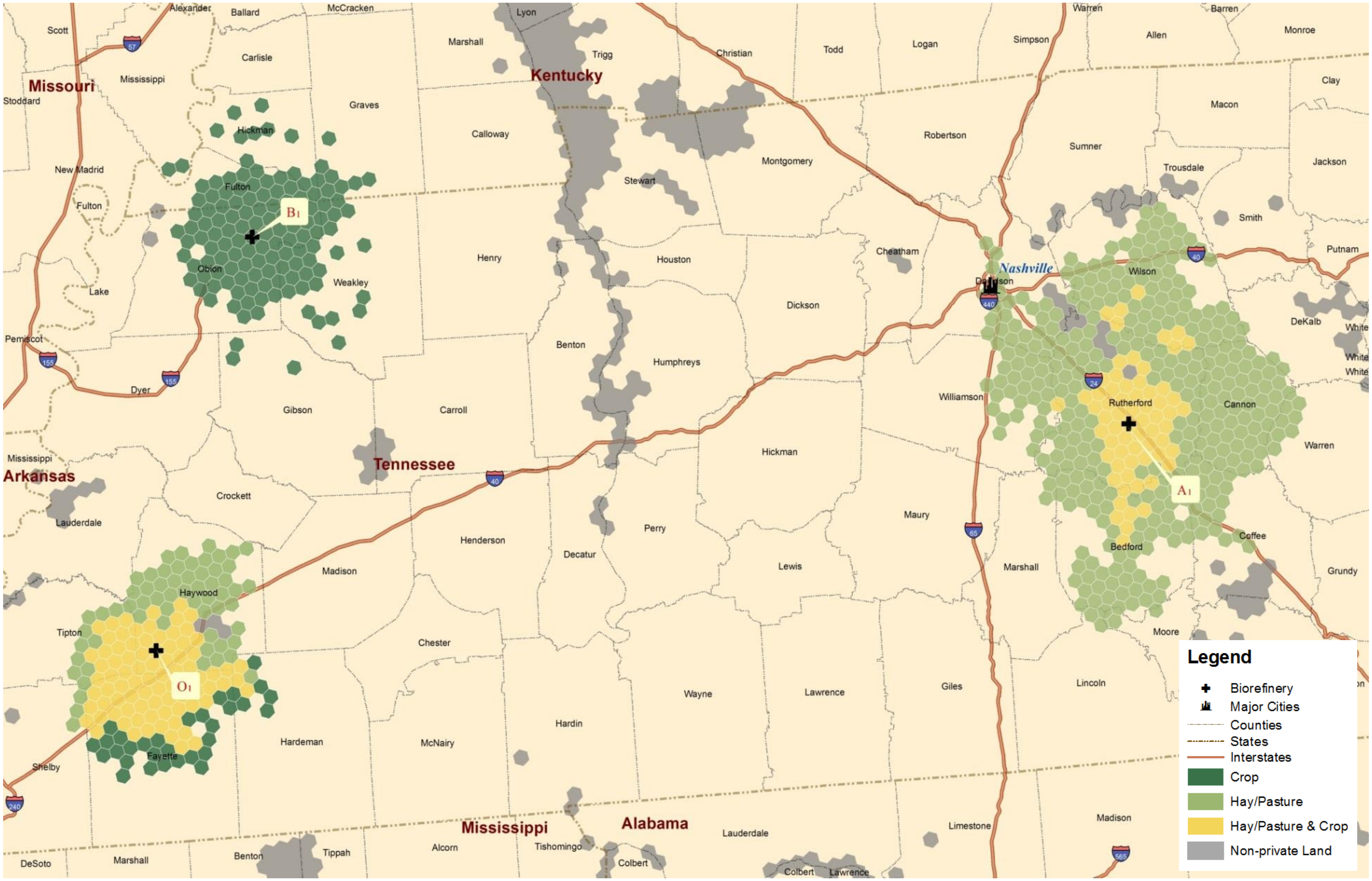

Figure 12. Location of biorefinery and associated supply region for three selected biorefinery candidates in scenario 1-a using square bale

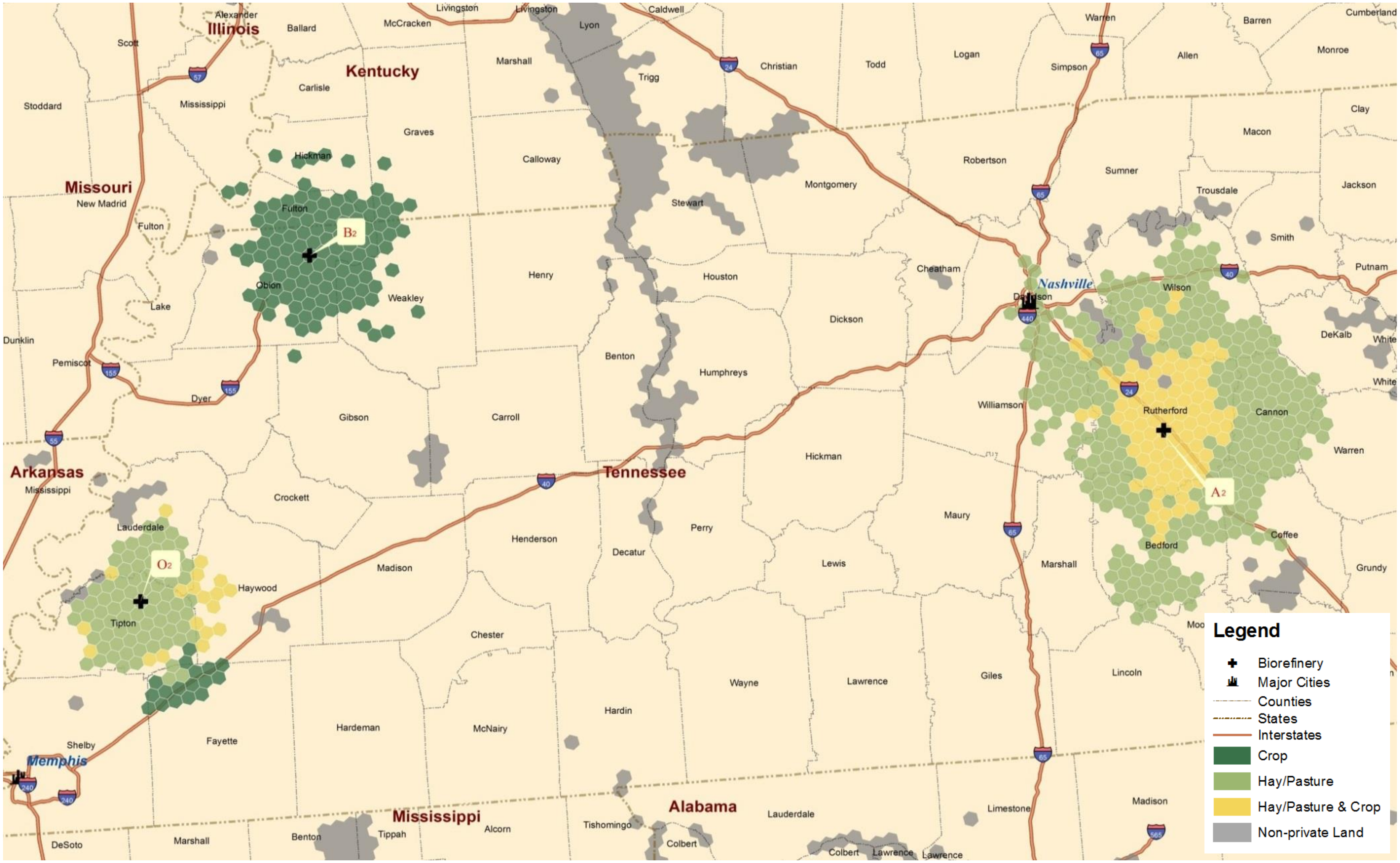

Figure 13. Location of biorefinery and associated supply regions for three selected biorefinery candidates in scenario 1-b using round bale

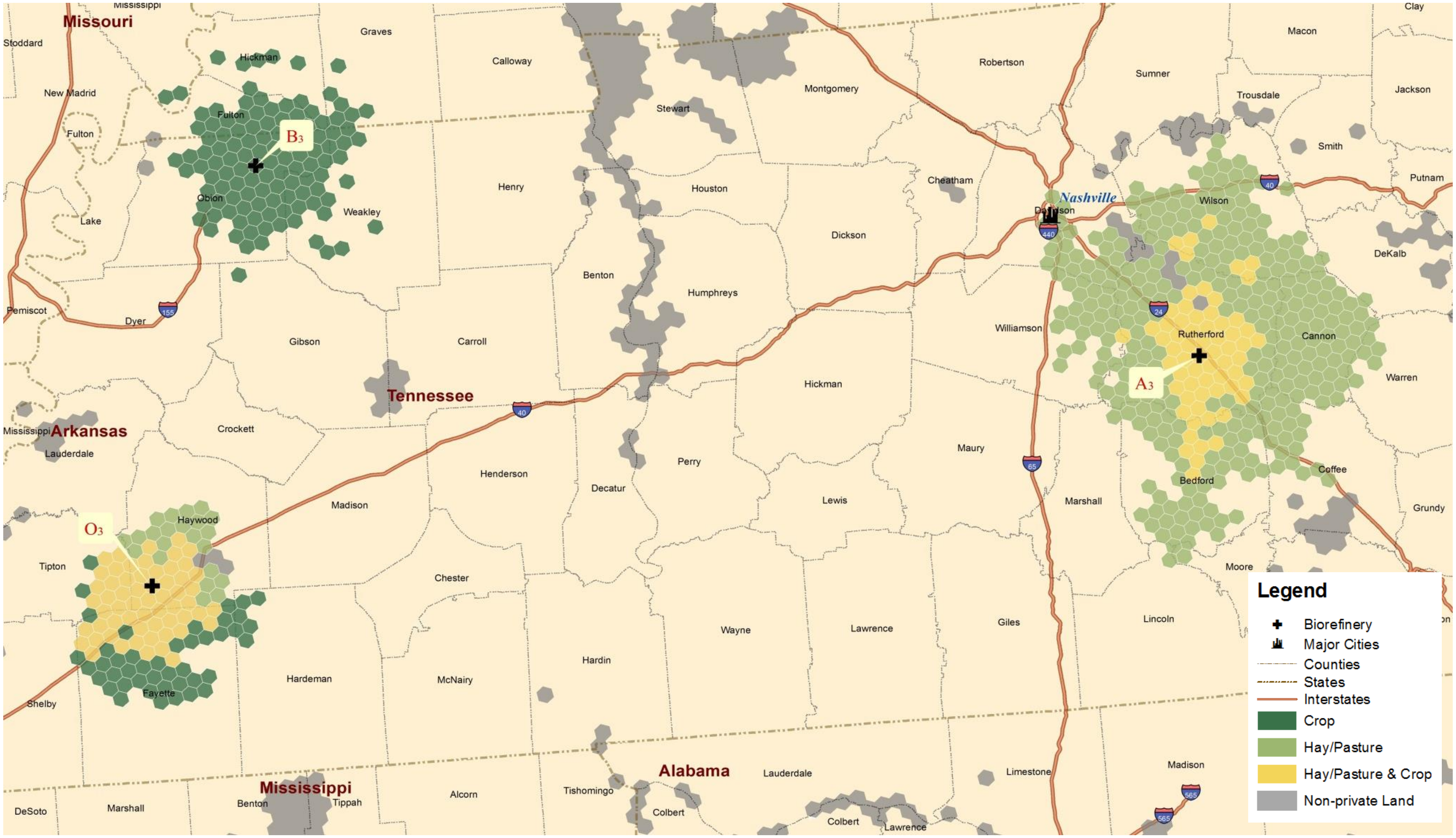

Figure 14. Location of biorefinery and associated supply region for three selected biorefinery candidates in scenario 1-c using square bale with no DML during storage

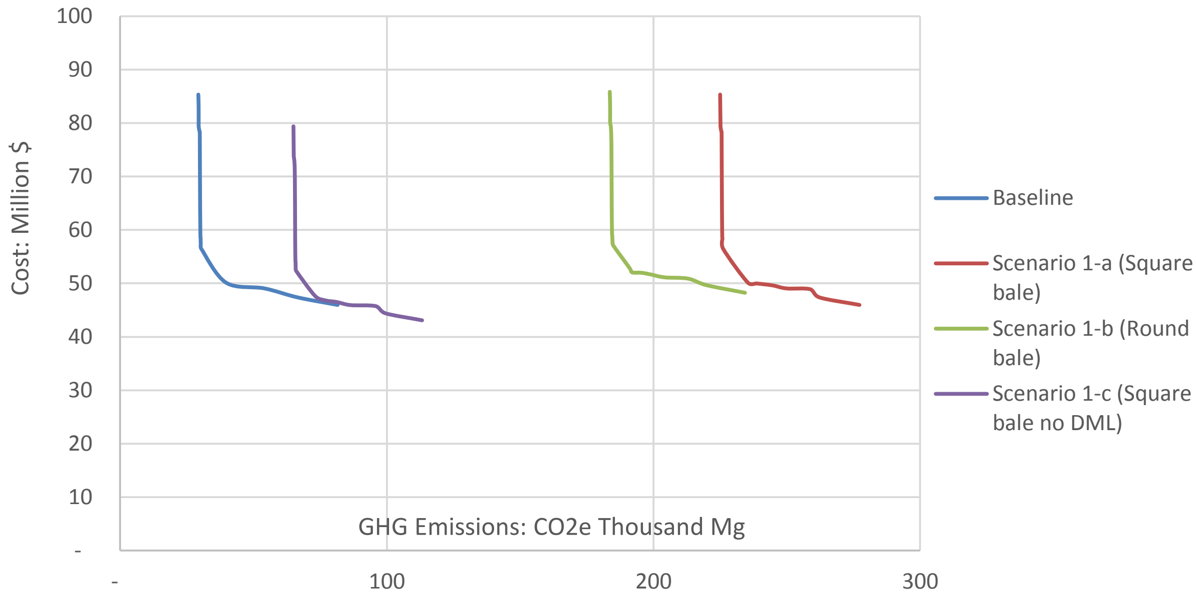

Figure 15. Regional tradeoff curves for baseline and the three cases in scenario 1

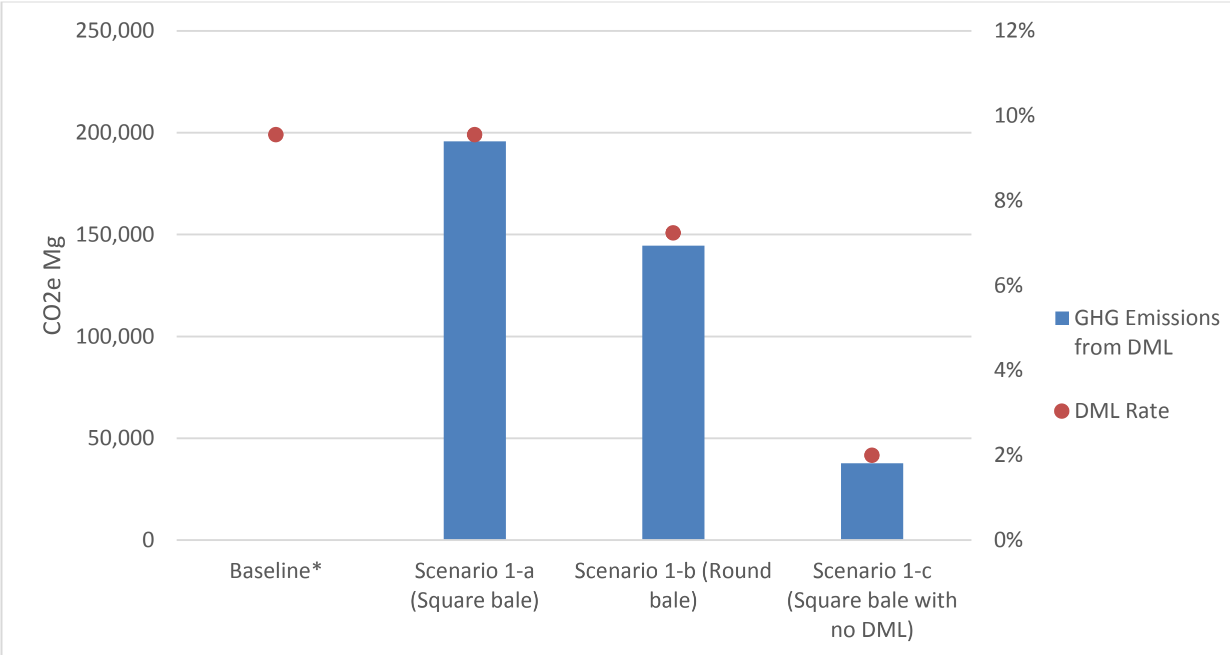

Figure 16. The DML rate and associated GHG emissions from baseline and three cases in scenario 1

Note: GHG emissions from DML decomposition were neglected in the baseline.

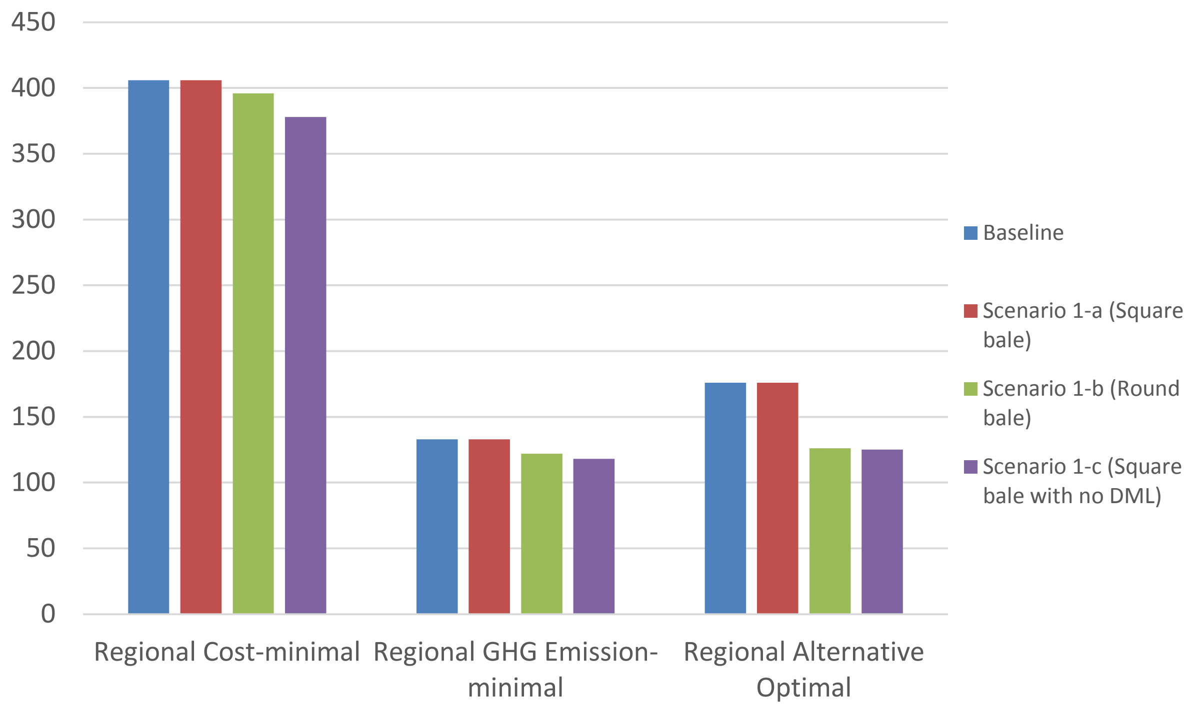

Figure 17. Number of crop zones converted for switchgrass production for baseline and the three cases in scenario 1

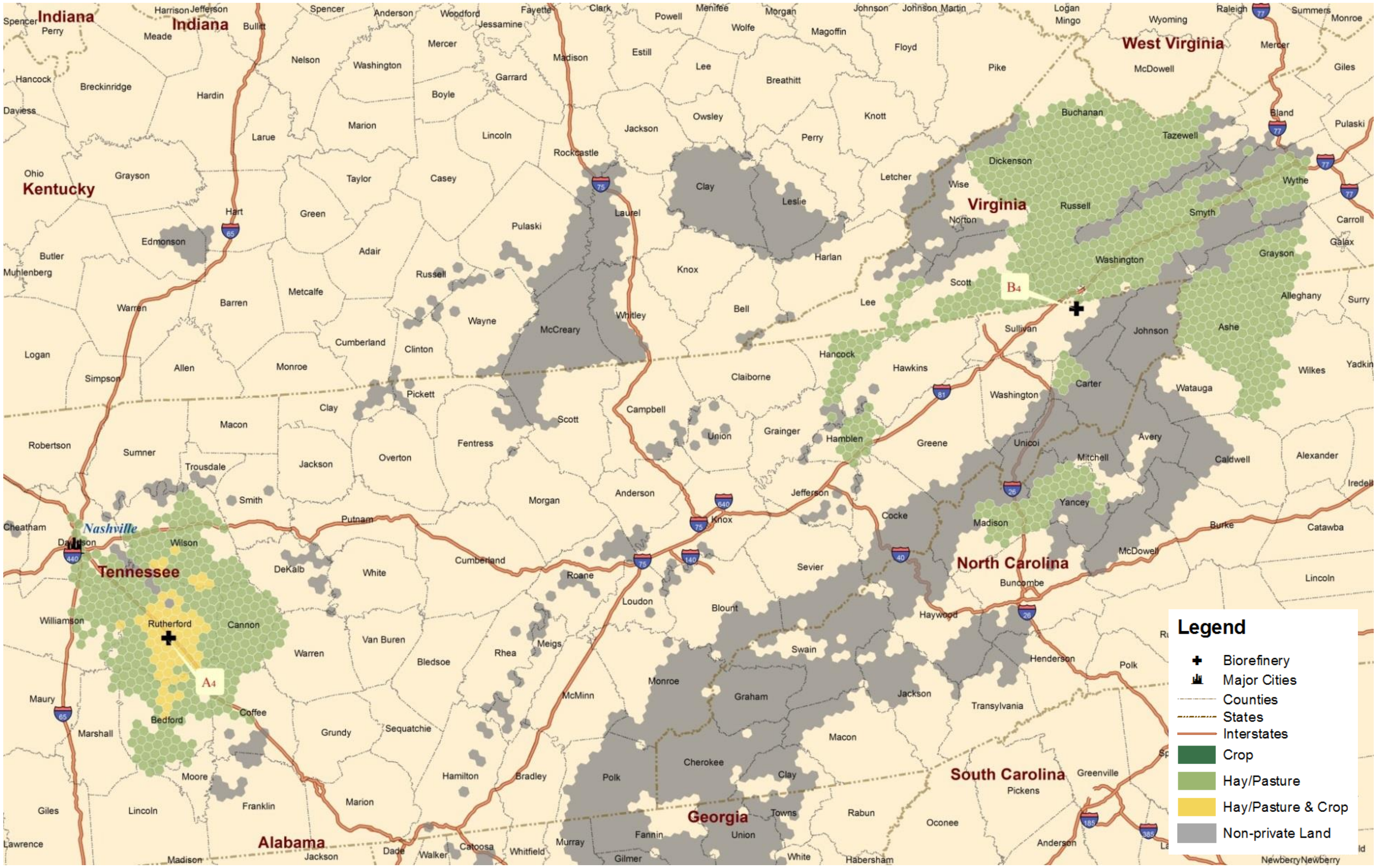

Figure 18. Location of biorefinery and associated supply region for regional cost-minimal (A4) and regional GHG emission-minimal (B4) biorefinery candidates in scenario 2-a with PAS_{hay} equals 50%

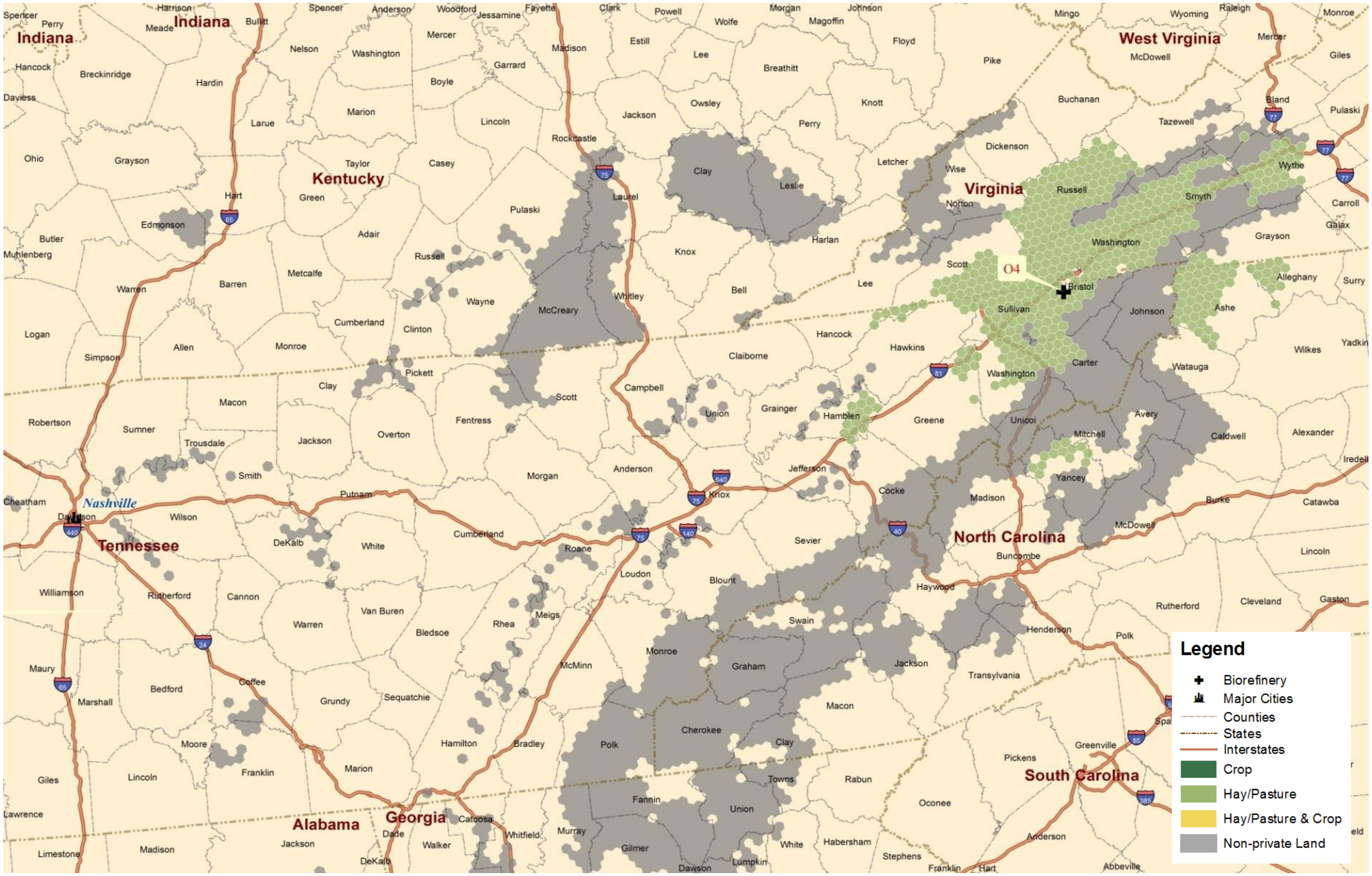

Figure 19. Location of biorefinery and associated supply region for the alternative optimal biorefinery candidate (O4) in scenario 2-a with PAS_{hay} equals 50%

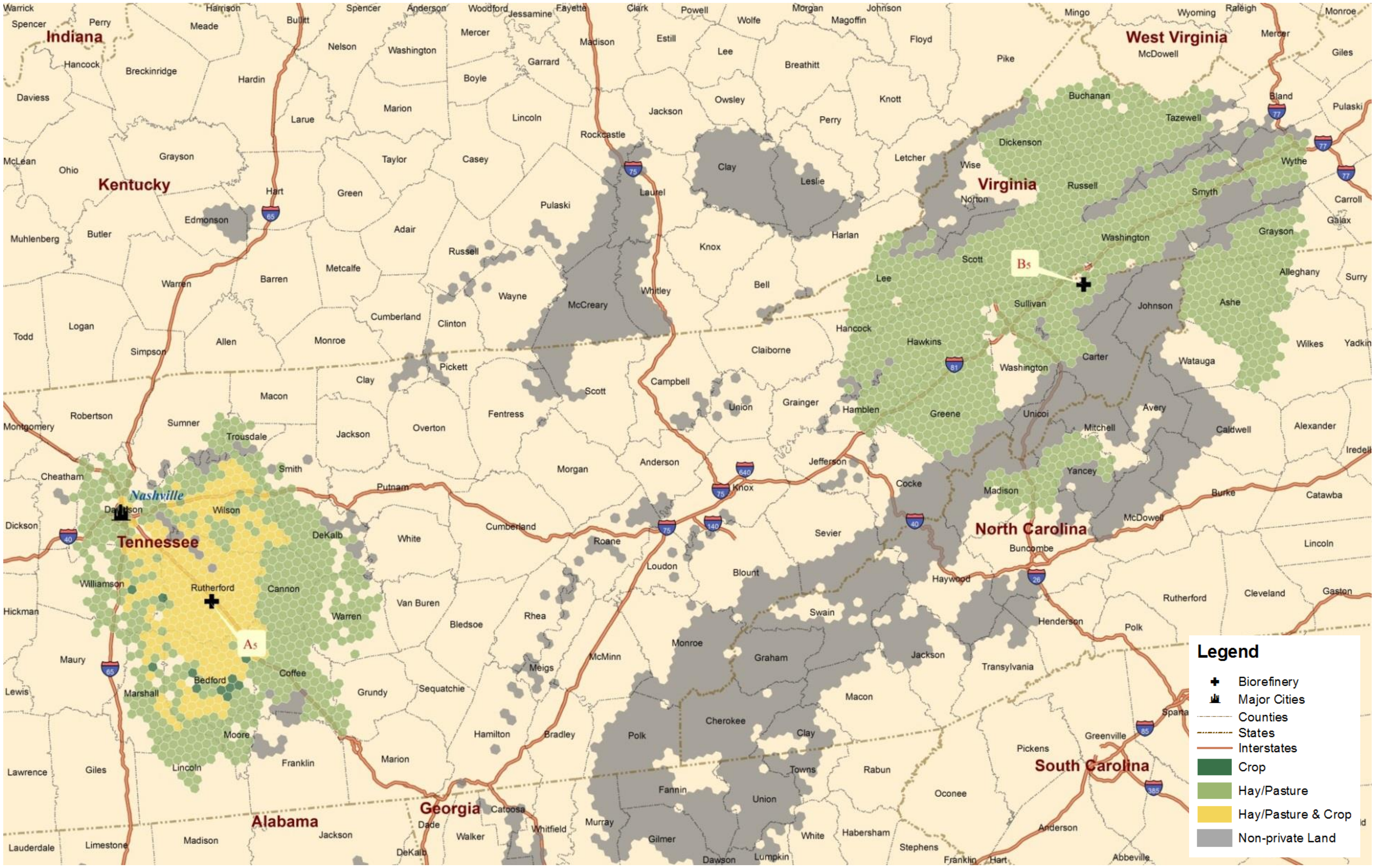

Figure 20. Location of biorefinery and associated supply region for regional cost-minimal (A5) and regional GHG emission-minimal (B5) biorefinery candidates in scenario 2-b with PAS_{hay} equals 25%

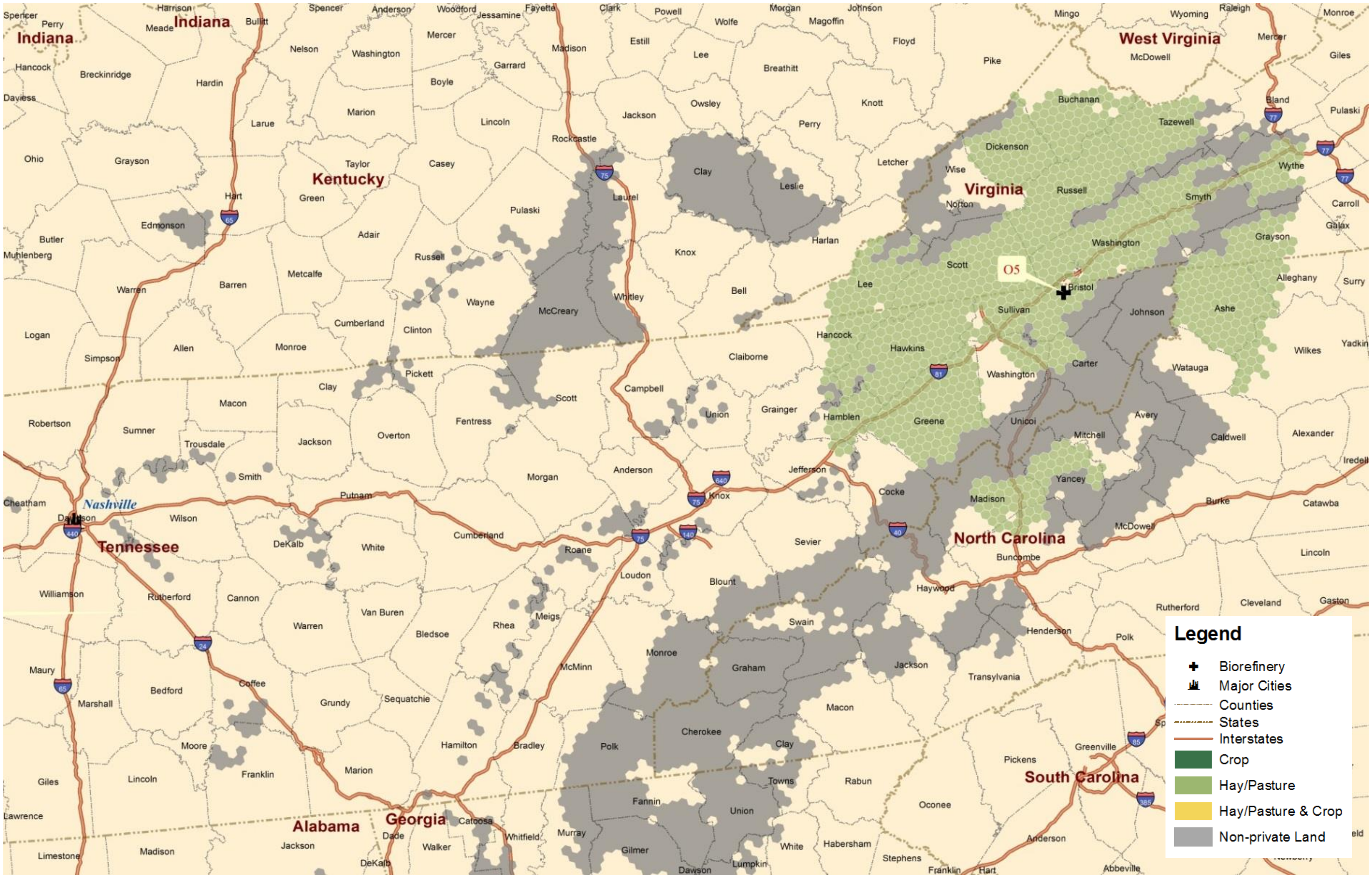

Figure 21. Location of biorefinery and associated supply region for the alternative optimal biorefinery candidate (O5) in scenario 2-b with PAS_{hay} equals 25%

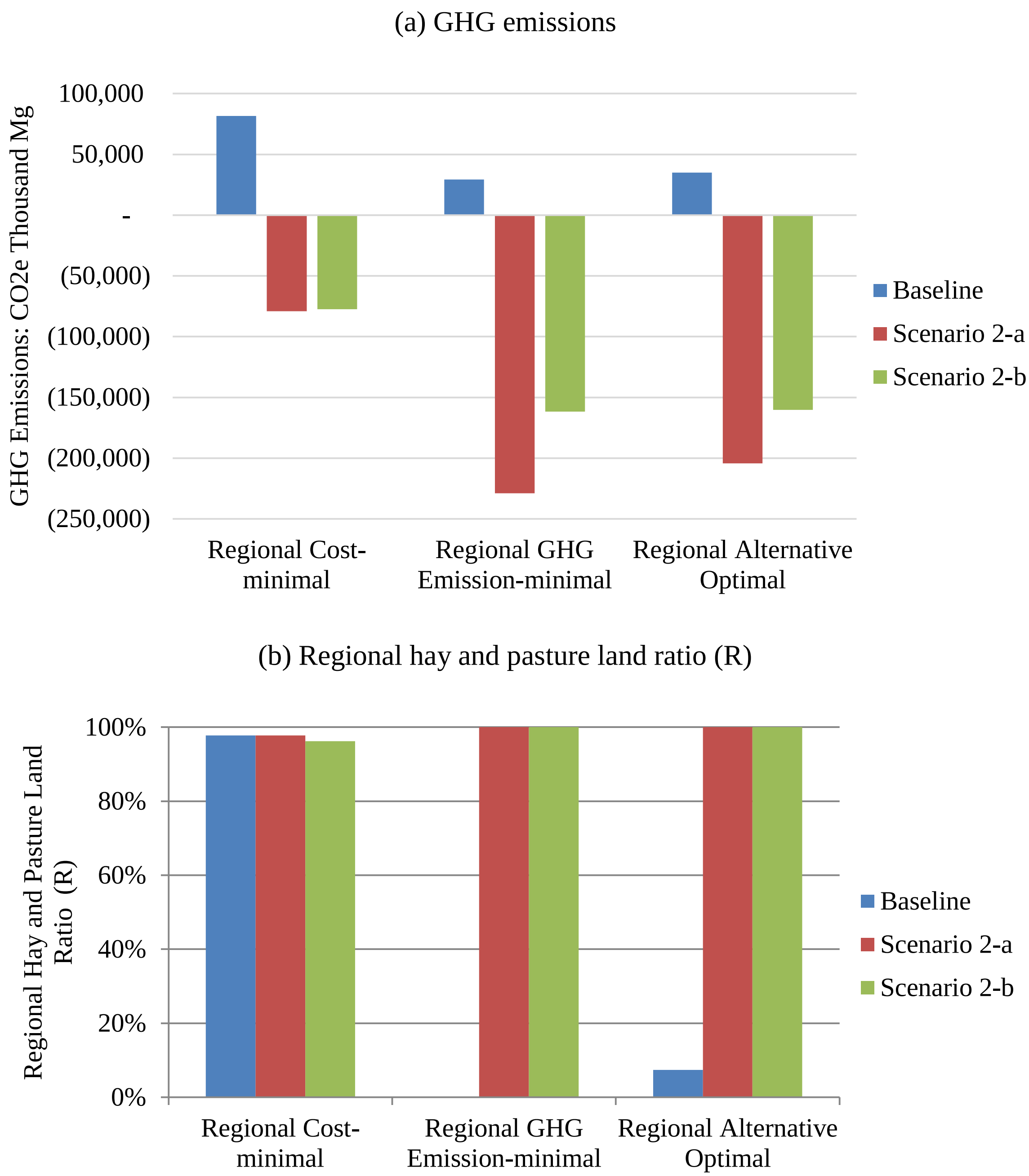

Figure 22. GHG emissions and associated R from the three selected biorefinery candidates for baseline and the two cases in scenario 2

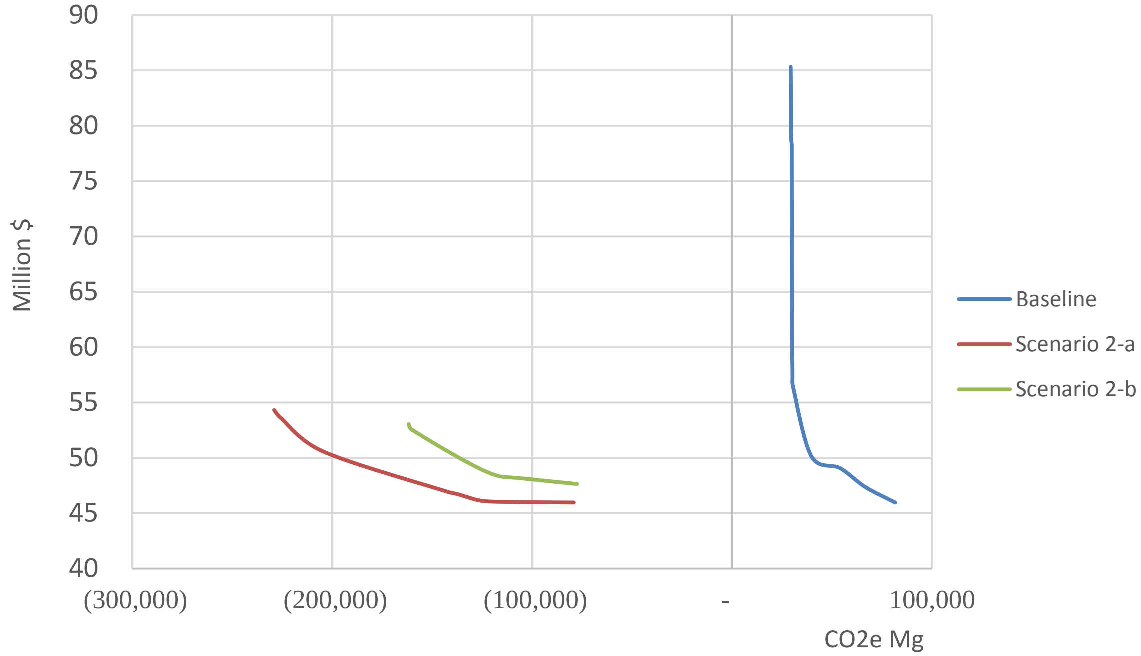

Figure 23. Regional tradeoff curves for baseline and the two cases in scenario 2

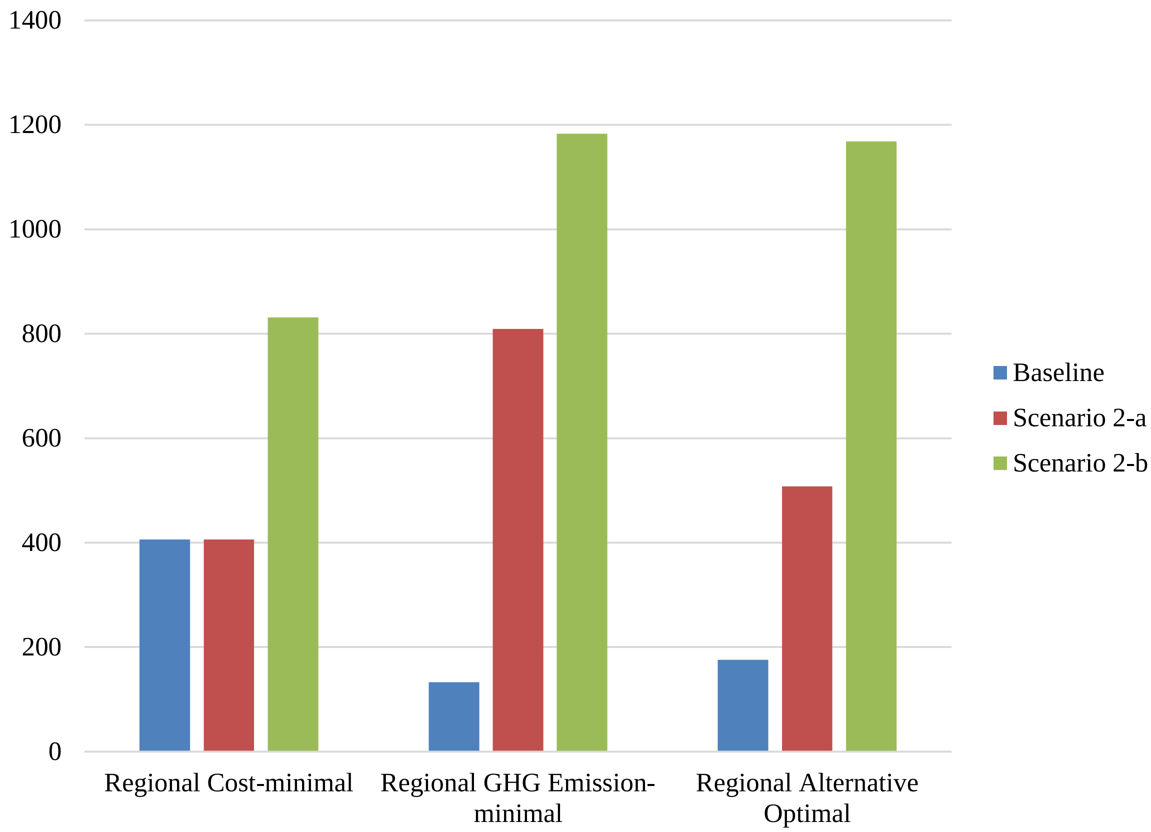

Figure 24. Number of crop zones converted for switchgrass production for baseline and the two cases in scenario 2

Vita

Zidong Wang was born on June 25, 1990 in Hubei, China. He graduated from Renmin University of China where he achieved his Bachelor's degree in Agricultural and Resource Economics in 2011. He is currently a graduate research assistant in the Department of Agricultural and Resource Economics at the University of Tennessee, Knoxville. He will obtain his Master of Science degree in Agricultural Economics in August, 2013. He has now accepted an offer to pursue his doctoral degree at Department of Agricultural Economics at Texas A&M University.